Math. Res. Lett.
Volume 29, Number 6, 1595–1658, 2022

Diagrams of $\star$-trisections

Román Aranda and Jesse Moeller

Communicated by the David Gabai

In this note we provide a generalization for the definition of a trisection of a 4-manifold with boundary. We demonstrate the utility of this more general definition by finding a trisection diagram for the Cacime Surface, and also by finding a trisection-theoretic way to perform logarithmic surgery. In addition, we describe how to perform 1-surgery on closed trisections. The insight gained from this description leads us to the classification of an infinite family of genus three trisections. We include an appendix where we extend two classic results for relative trisections for the case when the trisection surface is closed.

1. Introduction

In [14], Gay and Kirby proved that every closed smooth 4-manifold admits a trisection. A trisection of a closed 4-manifold X is a decomposition $X = X_1 \cup X_2 \cup X_3$ into three 4-dimensional 1-handlebodies so that the pairwise intersections are 3-dimensional 1-handlebodies $X_i \cap X_j$, and the triple intersection is a closed surface $\Sigma = X_1 \cap X_2 \cap X_3$. The genus of the trisection is defined as the genus of Σ. In recent years, the notion of trisections has been extended to 4-manifolds with several boundaries [7], knotted surfaces in 4-manifolds [24] and finitely presented groups [1]. See [18] for an exposition on recent advances in the theory of trisections of 4-manifolds.

The main goal of this paper is to introduce a generalization of trisections of 4-manifolds, called $\star$-trisections, and to develop the diagrammatics of this new theory. One dificulty of studying trisections of 4-manifolds is the rate at which the genus of the trisections grows under certain operations. Softening the definition of a trisection of a 4-manifold with boundary can potentially reduce this complexity. For example, in [9], a genus seven trisection of $T^2 \times S^2$ was obtained by taking the double of a genus 3 trisection for $T^2 \times D^2$. In Figure 18, we use a genus one $\star$-trisection for $T^2 \times D^2$ to draw a genus four trisection for $T^2 \times S^2$.

We generalize the definition of trisection by relaxing the definition of the 4-manifolds which make up the pieces of the trisection. The definition of $\star$-trisections can be found in Section 2. For the interested reader, in Section 3 we dedicate several remarks, lemmas, and figures to the exposition of these new 4-dimensional pieces which we use to build $\star$-trisections; we discuss two equivalent constructions of these pieces, and describe the boundary of a $\star$-trisected 4-manifold. The diagrammatics of these new $\star$-trisections are presented in Section 4.

In Sections 6 and 8, we show how to find $\star$-trisections for the complements of neighborhoods of certain embedded submanifolds. Motivated by [9], we prove a pasting lemma in Section 5 which allows us to glue two $\star$-trisected 4-manifolds along connected components of their boundaries. In Section 8 we use this pasting lemma explicitly to produce a closed trisection diagram for the Cacime Surface. In addition, we use the pasting lemma to decribe how to trisect the Fintushel-Stern knot surgery [12] and Logarithmic transforms in the spirit of [3].

Trisections of genus three

In [23], Meier and Zupan classified all trisections of genus at most two. It is therefore natural to seek a classification for trisections of low genus. As a proving ground, in this paper we study an infinite family of genus three trisection diagrams. Consider three rational numbers $\frac{a}{b}$, $\frac{c}{d}$, $\frac{p}{q}$ in reduced form. Let α_1 and α_2 be the top and middle curves of the left diagram in Figure 1 and let α_3 be the $\frac{a}{b}$ torus knot in the torus obtained by compressing along α_1 and α_2. Take α to be the union of these curves and define β and γ similarly using $\frac{c}{d}$ and $\frac{p}{q}$, respectively. Observe that (Σ, α, β) is a Heegaard diagram for $S^1 \times S^2$ or S^3 whenever $|ad - bc| \leq 1$. When this condition is satisfied for each pair of fractions, the tuple $(\Sigma; \alpha, \beta, \gamma)$ is a genus three trisection diagram. We call such tuple a Farey diagram $D(\frac{a}{b}, \frac{c}{d}, \frac{p}{q})$.

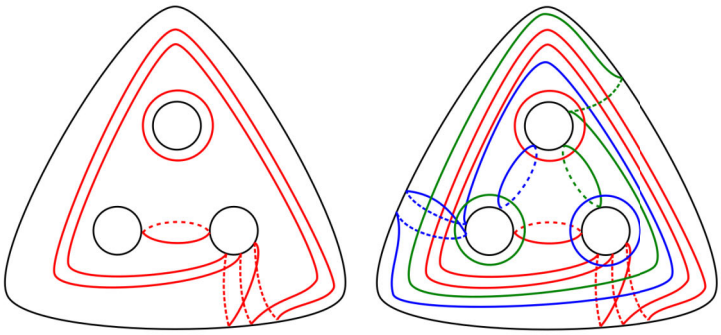

Figure 1: The Farey diagram $D(\frac{1}{1}, \frac{1}{2}, \frac{2}{3})$.

The problem of understanding Farey diagrams was proposed during the first day of the 2019 Spring Trisectors Meeting at UGA. By this time, progress had already been made on this problem in [21], where Meier showed that $D(\frac{q}{p}, \frac{q}{p}, \frac{q}{p})$ is the diagram of a spun lens space $L(p, q)$. Seeking a classification for genus three trisections, he conjectured the following.

Conjecture 1 (Meier [21]). Every irreducible 4-manifold with trisection genus three is either the spin of a lens space, or a Gluck twist on a specific 2-knot in the spin of a lens space.

In Section 7, we show that every Farey diagram is the result of pasting together ⋆-trisections for $S^2 \times D^2$ and $X - (S^1 \times B^3)$ along their boundaries, where $X \in \{S^1 \times S^3, S^4, \mathbb{CP}^2, \overline{\mathbb{CP}^2}\}$. In particular, Farey diagrams yield trisections for spun lens spaces or reducible 4-manifolds. We can further prove

that these diagrams are actually standard. Theorem 7.2, in conjunction with Meier's results on spun lens spaces, proves Conjecture 1 for the family of Farey trisections.

Theorem 7.2. Let $\{\frac{a}{b}, \frac{c}{d}, \frac{p}{q}\} \subset \mathbb{Q} \cup \{\frac{1}{0}\}$ with $d(x,y) \leq 1$ for each $x, y \in \{\frac{a}{b}, \frac{c}{d}, \frac{p}{q}\}$. If at least two of these fractions are distinct, then $D(\frac{a}{b}, \frac{c}{d}, \frac{p}{q})$ is equivalent to the standard diagram for $T \# S$ where $T \in \{S^4, \mathbb{CP}^2, \overline{\mathbb{CP}^2}\}$ and $S \in \{S^2 \times S^2, S^2 \widetilde{\times} S^2\}$.

Classic relative trisections

It is worthy of note that the current work on trisections of 4-manifolds with boundary is restricted to the case of the trisection surface having non-empty boundary. Besides a few remarks in the original trisections paper, not much has been said in the closed case. In order to complete the discussion of the basic theory of trisections of manifolds with boundary, in Appendix A we offer adaptations of proofs of the main theorems in [5] and [7] by Castro, Gay, and Pinzón-Caicedo. We prove that the algorithm which recovers the monodromy $\phi : P \to P$ of the induced circular structure $\partial X = P \times_\phi S^1$ also works in the case where P is a closed surface, and extend the algorithm to obtain a relative trisection from a Kirby diagram of X and a page of an open book decomposition (or fibration over S^1) on ∂X within the diagram.

2. Trisections of 4-manifolds

This section will be broken into two parts. In the first part, we will review the original definition of a 4-manifold trisection given by Gay and Kirby in [14]. We elaborate slightly on the definition by giving an equivalent definition involving 3-dimensional compression bodies as well as by including a description of the induced decomposition of the boundary in the relative case. This elaboration will assist in our exposition of $\star$-trisections. We formally introduce $\star$-trisections in the second part of this section.

2.1. Original definitions for trisections

A trisection of a closed, connected 4-manifold X is a decomposition of X into three 4-dimensional 1-handlebodies $X = X_1 \cup X_2 \cup X_3$ such that for each pair $i \neq j$ the intersection $X_i \cap X_j$ is a 3-dimensional handlebody and the common intersection $X_1 \cap X_2 \cap X_3$ is a closed surface. Here we offer an equivalent definition through the lens of viewing the 4-dimensional pieces in

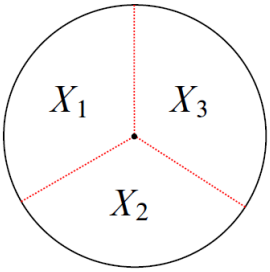

Figure 2: A picture two-dimensions lower of a trisection.

Figure 2 as thickened 3-dimensional handlebodies. Let C_k be a 3-dimensional handlebody with boundary a closed surface of genus k, F_k. Let $Z_k = [0,1] \times C_k \approx \natural_k \left(S^1 \times B^3\right)$. The boundary of Z_k admits a Heegaard splitting $Y_k = \partial Z_k = Y_k^+ \cup Y_k^-$ where

(1)
$$Y_k^+ = ([1/2,1] \times \partial F_k) \cup (\{1\} \times C_k) \text{ and } Y_k^- = (\{0\} \times C_k) \cup ([0,1/2] \times F_k)\,.$$

Given an integer $g \geq k$, let $Y_k = Y_{k,g}^+ \cup Y_{k,g}^-$ be the standard genus g Heegaard splitting of Y_k obtained by stabilizing the genus k Heegaard splitting $g-k$ times.

Definition 2.1 (Trisection of closed 4-manifold). A trisection of a closed, connected 4-manifold X is a splitting $X = X_1 \cup X_2 \cup X_3$ and integers $0 \leq k, n, g$ with $n \leq k \leq g$ such that each X_i is diffeomorphic to Z_k via a diffeomorphism $\varphi_i : X_i \to Z_k$ for which $\varphi_i(X_i \cap X_{i+1}) = Y_{k,g}^+$ and $\varphi_i(X_i \cap X_{i-1}) = Y_{k,g}^-$.

Notice that Z_k is a 4-dimensional 1-handlebody and the pairwise intersections $X_i \cap X_j$ are 3-dimensional handlebodies of genus g. This definition is just a slightly more technical rewording of the original presented at the beginning of the section. In [14], Gay and Kirby generalize this definition to allow 4-manifolds which have surface bundles over S^1 as boundary. We will again present this definition by presenting the wedges of the trisection as thickened 3-dimensional pieces.

For integers $k, b \geq 0$, let $F_{k,b}$ be a connected orientable surface of genus k with b boundary components. Fix non-negative integers b, k and n with $n < k$ and let $C_{k,b,n}$ denote a 3-dimensional compression body with $F_{k,b}$

as the positive boundary and with $F_{k-n,b}$ as the negative boundary. This compression body is built by attaching n 3-dimensional 2-handles to $\{1\} \times F_k \subset [0,1] \times F_k$, yielding a cobordism from $F_{k,b}$ to $F_{k-n,b}$. Now consider the 4-manifold $Z_{k,b,n} := [0,1] \times C_{k,b,n}$. Part of $\partial Z_{k,b,n}$ is

$$Y_{k,b,n} := (\{0\} \times C_{k,b,n}) \cup ([0,1] \times F_{k,b}) \cup (\{1\} \times C_{k,b,n}), \tag{2}$$

which has a natural genus k Heegaard splitting into two compression bodies

$$Y^+_{k,b,n} := ([1/2,1] \times F_{k,b}) \cup (\{1\} \times C_{k,b,n}), \tag{3}$$

$$Y^-_{k,b,n} := (\{0\} \times C_{k,b,n}) \cup ([0,1/2] \times F_{k,b}). \tag{4}$$

Finally, given any $g \geq k$, let $Y_{k,b,n} = Y^+_{k,b,n,g} \cup Y^-_{k,b,n,g}$ be the genus g Heegaard splitting obtained from the natural genus k splitting by stabilizing $g-k$ times.

Definition 2.2 (Relative trisection). A trisection of a connected 4-manifold X with non-empty connected boundary is a splitting $X = X_1 \cup X_2 \cup X_3$ and integers $0 \leq k, b, n, g$ with $n < k \leq g$ such that each X_i is diffeomorphic to $Z_{k,b,n}$ via a diffeomorphism $\varphi_i : X_i \to Z_{k,b,n}$ for which

$$\varphi_i(X_i \cap X_{i+1}) = Y^+_{k,b,n,g} \text{ and } \varphi_i(X_i \cap X_{i-1}) = Y^-_{k,b,n,g}.$$

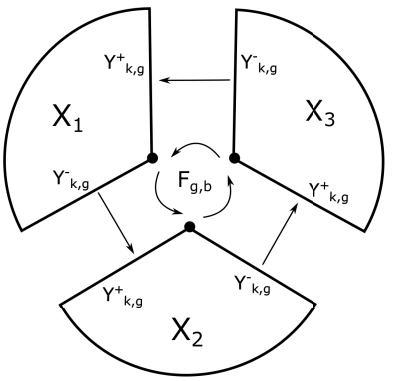

Figure 3: A (relative) trisected 4-manifold is built by gluing three standard 4-dimensional pieces along submanifolds of their boundary.

We can interpret a 3-dimensional handlebody C_k as a cobordism from a closed surface F_k to the empty set. This way, Definition 2.2 generalizes Definition 2.1. For a detailed discussion on the properties of relative trisections

one can see [5, 7, 14]. The authors of this paper like to think of trisections of 4-manifolds as decompositions into three 'standard' pieces Z_i glued along submanifolds of their boundary. In this paper we will see some interactions between relative and $\star$-trisections. In the following subsection we will describe the standard models for the 4-manifold pieces in a $\star$-trisection.

2.2. $\star$-Trisections of 4-manifolds

Here we will define a more general definition of 4-manifold trisection, which we call $\star$-trisection, by first defining analogous 4-dimensional wedges and then gluing these along submanifolds of their boundaries. Informally, these are obtained by gluing two copies of the 4-manifolds $Z_{k,b,n}$ in Subsection 2.1, and removing properly embedded 2-disks in a controlled way.

Let $F_+ = F_{k,b}$ and $F_- = \dot{\bigcup}_{i=1}^{s} F_{k_i,b_i}$ be two orientable surfaces with $k \geq \sum k_i$, $b = \sum b_i$ and $s \geq 0$. F_+ is a connected surface and F_- has $s \geq 0$ connected components. We will always assume that F_- has no 2-sphere components. Let C be a 3-dimensional connected compression body with positive boundary $\partial_+ C = F_+$ and negative boundary $\partial_- C = F_-$. This compression body is obtained by attaching 3-dimensional 2-handles to $F_+ \times \{1\} \subset F_+ \times [0,1]$, and capping-off the resulting 2-sphere components with 3-handles. This produces a cobordism C from F_+ to F_-. The 2-handles above are attached along a collection of pairwise disjoint, non isotopic and possibly boundary parallel simple closed curves $\delta \subset F_+$.

Let $\widetilde{C}$ be a compression body with positive boundary F_{k,b_0}. Consider $\widetilde{C}^0, \widetilde{C}^1 \subset \widetilde{C}$ two sub-compression bodies spanning $\widetilde{C}$ with common part a sub-compression body $\widetilde{C}_{all}$; i.e., $\widetilde{C}$ is built using a collection of pairwise disjoint simple closed curves $\widetilde{\delta} \subset F_{k,b_0}$ such that $\widetilde{\delta} = \delta^0 \cup \delta^1$, $\delta_{all} = \delta^0 \cap \delta^1$ with $\widetilde{C}^i$ determined by δ^i and $\widetilde{C}_{all}$ determined by δ_{all}. Define

$$\widetilde{Z} = \widetilde{C}^0 \times [0,1/2] \bigcup_{\widetilde{C}_{all} \times \{1/2\}} \widetilde{C}^1 \times [1/2,1]. \tag{5}$$

Consider the submanifold of $\partial \widetilde{Z}$,

$$\widetilde{Y} = \left(\widetilde{C}^0 \times \{0\}\right) \cup (F_{k,b_0} \times [0,1]) \cup \left(\widetilde{C}^1 \times \{1\}\right). \tag{6}$$

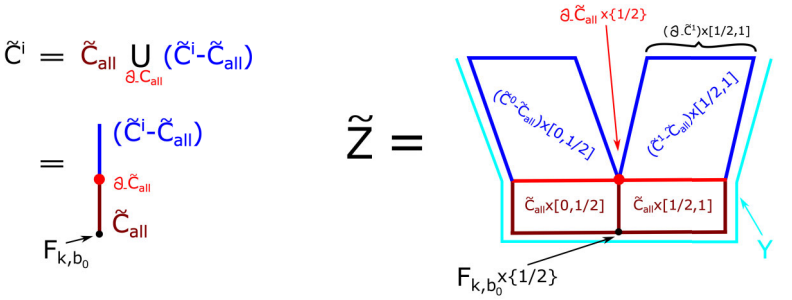

Figure 4: A diagram of $\widetilde{Z}$ two dimensions down.

Both $\partial\widetilde{Z}$ and $\widetilde{Y}$ are connected 3-manifolds. Moreover, the surface $F_{k,b_0} \times \{1/2\}$ determines a natural Heegaard splitting of $\widetilde{Y} = \widetilde{Y}_+ \cup \widetilde{Y}_-$ given by

$$\begin{aligned} \widetilde{Y}_- &= \left(\widetilde{C}^0 \times \{0\}\right) \cup (F_{k,b_0} \times [0,1/2]) \\ \text{and } \widetilde{Y}_+ &= (F_{k,b_0} \times [1/2,1]) \cup \left(\widetilde{C}^1 \times \{1\}\right). \end{aligned} \tag{7}$$

Define Z to be the 4-manifold obtained from $\widetilde{Z}$ by attaching $m \geq 0$ 1-handles with both feet in $\widetilde{Y}$. Equivalently, Z is obtained by carving a collection of boundary parallel 2-dimensional disks $(D, \partial D) \subset (\widetilde{Z}, \widetilde{Y})$. We will prove in Lemma 3.5 that there is a unique isotopy class of boundary parallel disks in $\widetilde{Z}$ with a given boundary. Thus the boundary link $U = D \cap \widetilde{Y}$ is an unlink of unknots determining the collection D. Isotope U in bridge position with respect to the Heegaard splitting $\widetilde{Y} = \widetilde{Y}_- \cup \widetilde{Y}_+$; this means that $U \cap \left(\widetilde{C}^i \times \{i\}\right)$ is a collection of boundary parallel arcs on each compression body, and $U \cap (F_{k,b_0} \times [0,1])$ is a colection of product arcs.

Set $C^i = (\widetilde{C}^i \times \{1/2\}) - \eta(U)$, $Y = \widetilde{Y} - \eta(U)$ and $Z = \widetilde{Z} - \eta(D)$. By construction C^0 and C^1 are compression bodies with positive boundary the surface $F_{k,b} = F_{k,b_0} - \eta(U)$ with $b := b_0 + |U \cap (F_{k,b_0} \times \{1/2\})|$. Furthermore, $Y \subset Z$ is given by

$$Y = Y_{C^0,C^1} := \left(C^0 \times \{0\}\right) \cup (F_{k,b} \times [0,1]) \cup \left(C^1 \times \{1\}\right), \tag{8}$$

which admits a Heegaard splitting $Y_{C^0,C^1} = Y^+_{C^0,C^1} \cup Y^-_{C^0,C^1}$ as follows

$$\begin{aligned} Y^+_{C^0,C^1} &:= (F_{k,b} \times [1/2,1]) \cup \left(C^1 \times \{1\}\right) \\ Y^-_{C^0,C^1} &:= \left(C^0 \times \{0\}\right) \cup (F_{k,b} \times [0,1/2]) \end{aligned}$$

For $g \geq k$, let $Y_{C^0,C^1} = Y^+_{C^0,C^1;g} \cup Y^-_{C^0,C^1;g}$ be the splitting above stabilized $g-k$ times. In the next section we will see that the 4-manifold Z can be built from the information of C^0, C^1 and C_{all}, where C_{all} is the common compression body between C^0 and C^1 obtained by embedding the loops $\widetilde{\delta}_{all}$ into Σ and adding some new loops from U (see Remark 3.8). Thus we write $Z = Z(C^0, C^1, C_{all})$ to emphasize this dependence.

Definition 2.3 ($\star$-Trisection). A $\star$-trisection of a connected 4-manifold X is a decomposition $X = X_1 \cup X_2 \cup X_3$ with connected compression bodies $C^0_{(i)}$, $C^1_{(i)}$, $C_{(i),all}$ as above and an integer $g \geq g(\partial_+ C^j_{(i)})$ for $i = 1, 2, 3$, $j = 0, 1$, such that each X_i is diffeomorphic to $Z(C^0_{(i)}, C^1_{(i)}, C_{(i),all})$ via a map $\varphi_i : X_i \to Z(C^0_{(i)}, C^1_{(i)}, C_{(i),all})$ for which

$$\varphi_i(X_i \cap X_{i+1}) = Y^+_{C^0_{(i)},C^1_{(i)};g} \text{ and } \varphi_i(X_{i-1} \cap X_i) = Y^-_{C^0_{(i)},C^1_{(i)};g}.$$

The triple intersection is a connected surface Σ of genus g with $b \geq 0$ boundary components called the $\star$-trisection surface.

Remark 2.4 (Classic trisections). If all of the compression bodies $C^j_{(i)}$ have empty negative boundary, each $Y^{\pm}_{C^0_{(i)},C^1_{(i)};g}$ is a handlebody and it follows that X is closed. Here, the definition above agrees with the original definition of a trisection when X is closed [14]. If for all i we have that $C^0_{(i)}$ and $C^1_{(i)}$ are compression bodies determined by the same loops with connected negative boundary or $Y^{\pm}_{C^0_{(i)},C^1_{(i)};g}$ are determined by the curves in Figure 5 of [7], then this decomposition is the same as a trisection of a 4-manifold with boundary in [5, 7, 14]. Such trisections induce an open book decomposition on ∂X with binding a b-component link. We will refer to all the above as **classical trisections**, among them we refer to the ones with $\partial X \neq \emptyset$ as **relative trisections**. We will sometimes wish to distinguish whether or not the binding of the open book ∂X is empty; in these cases we will simply write $b = 0$ or $b > 0$, referring to the number of boundary components on the relative trisection diagram. The most general trisection, or **$\star$-trisection**, is when $C^0_{(i)}$ is not the same as $C^1_{(i)}$ for some i. The following section is dedicated to present different ways of thinking about the sectors of $\star$-trisections.

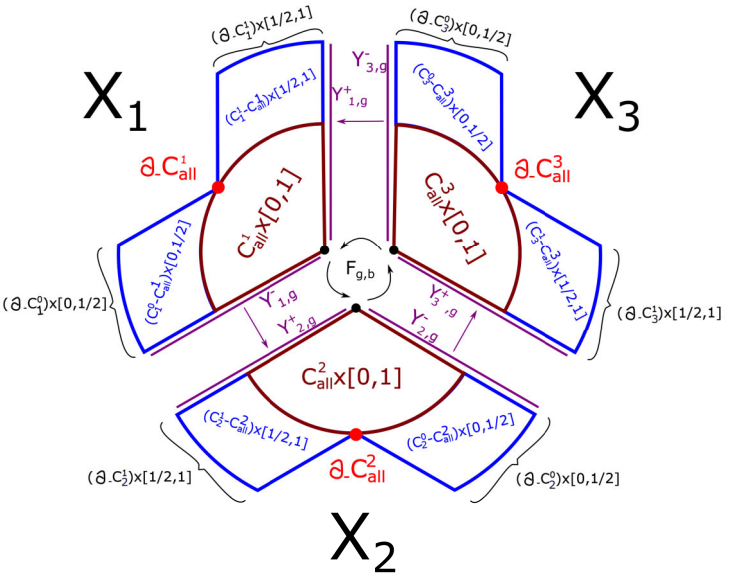

Figure 5: A $\star$-trisected 4-manifold X is built by gluing three 'standard' 4-dimensional pieces $Z(C^0_{(i)}, C^1_{(i)}, C_{(i),all})$ $(i = 1, 2, 3)$ along submanifolds of their boundary. Notice that if for each i the compression bodies $C^0_{(i)}$ and $C^1_{(i)}$ are determined by the same sets of curves, then the extra 'blue fins' in the diagram disapear, giving us a foliation of the boundary of X by copies of $\partial_- C_{(1),all}$.

3. The standard pieces

In this section we will describe two equivalent ways of building the 'standard' 4-dimensional piece $Z(C^0_{(i)}, C^1_{(i)}, C_{(i),all})$ of a $\star$-trisection. The first construction presents these standard pieces as boundary-connected sums of simple 4-dimensional blocks and also establishes the uniqueness of the boundary parallel disks in $\widetilde{Z}$, which are carved to form Z, up to isotopy. The second construction presents these standard pieces from the handlebody perspective. Remarks 3.8 and 3.9 summarize the conclusions of this section in the form of four equations (15-18) and a description of the types of curves needed to build a 'standard piece'.

Notation. Let $\widetilde{C}$ be a compression body with positive boundary F_{k,b_0}. Consider $\widetilde{C}^0, \widetilde{C}^1 \subset \widetilde{C}$ two sub-compression bodies spanning $\widetilde{C}$ with fixed common part a sub-compression body $\widetilde{C}_{all}$; i.e., there is a collection of simple closed curves $\widetilde{\delta} \subset F_{k,b_0}$ determining $\widetilde{C}$ such that $\widetilde{\delta} = \delta^0 \cup \delta^1$, $\delta_{all} = \delta^0 \cap \delta^1$

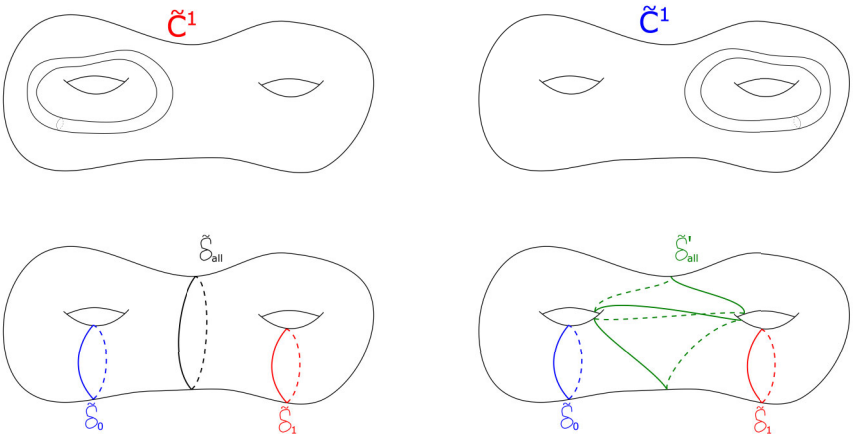

Figure 6: Example of loops determining the compression bodies $\widetilde{C}^i$, $\widetilde{C}_i$, and $\widetilde{C}_{all}$. Note in this case $\widetilde{C}$ is a handlebody and $\widetilde{\delta}_0 \cup \widetilde{\delta}_1 \cup \widetilde{\delta}_{all}$ is not a minimal set of meridians for $\widetilde{C}$. The bottom part shows two distinct chioces for loops in $\widetilde{\delta}_{all}$.

with $\widetilde{C}^i$ determined by δ^i and $\widetilde{C}_{all}$ determined by δ_{all}. Denote by $\widetilde{F}_{all}$ the negative boundary of $\widetilde{C}_{all}$. Denote by $\widetilde{C}_i = \widetilde{C}^i - int(\widetilde{C}_{all})$. $\widetilde{C}_i$ is a (possibly disconnected) compression body with positive boundary $\widetilde{F}_{all}$ determined by the curves[1] $\widetilde{\delta}_i = \widetilde{\delta}^i - \widetilde{\delta}_{all}$.

We will always choose $\widetilde{\delta}_i$ such that the following condition is satisfied: when compressing each component of $\widetilde{F}_{all}$ along $\widetilde{\delta}_i$, the resulting surface will have at most one sphere component; with equality if and only if the component of $\widetilde{C}_i$ is a handlebody. In particular we will always be able to build $\widetilde{C}_{all}$ with no 3-handles unless $\widetilde{F}_{all}$ is empty and $\widetilde{C}_{all}$ is a handlebody.

Remark 3.1 (Non-uniqueness of $\widetilde{C}_{all}$). Given two compression bodies $\widetilde{C}^0, \widetilde{C}^1 \subset \widetilde{C}$, the compression body $\widetilde{C}_{all}$ is not uniquely determined up to isotopy inside $\widetilde{C}$. This can be seen by taking the 3-manifold with the Heegaard splitting $W = C^0 \cup_{F_{k,b_0}} C^1$. Separating loops in $\widetilde{\delta}_{all}$ come from separating spheres in W, which might not be isotopic depending on the topology of W. The bottom part of Figure 6 shows an example of distinct $\widetilde{\delta}_{all}$ sets.

[1]The curves $\widetilde{\delta}_i$ in F_{k,b_0} can also be drawn in F_{all} since they are disjoint from $\widetilde{\delta}_{all}$.

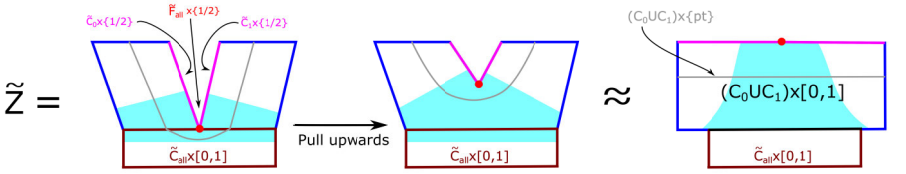

Figure 7: How to pull $\widetilde{F}_{all} \times \{1/2\}$ 'up'. Notice that the isotopy has support in a subset of $\widetilde{Z}$ diffeomorphic to $\widetilde{F}_{all} \times E$, where E is the shaded disk.

3.1. Construction 1

Using Figure 4, we can convince ourselves that $\widetilde{Z}$ can be built from $\widetilde{C}_{all} \times [0,1]$ by gluing collars of the subcompression bodies C_i. More precisely,

$$\widetilde{Z} \;=\; \widetilde{C}_0 \times [0,1/2] \bigcup_{\widetilde{F}_{all} \times [0,1/2]} \widetilde{C}_{all} \times [0,1] \bigcup_{\widetilde{F}_{all} \times [1/2,1]} \widetilde{C}_1 \times [1/2,1]. \tag{9}$$

We think of the product regions $\widetilde{C}_0 \times [0,1/2]$ and $\widetilde{C}_1 \times [1/2,1]$ as 'fins' attached to $\widetilde{C}_{all} \times [0,1]$, with the interval directions being horizontal in Figure 4. Imagine pulling $\widetilde{F}_{all} \times \{1/2\}$ 'up' in order to horizontally align the fibers $\widetilde{C}_i \times \{pt\}$ of the fins (see Figure 7). This makes the interval directions for the product regions $\widetilde{C}_0 \times [0,1/2]$ and $\widetilde{C}_1 \times [1/2,1]$ now vertical in the figure. Such isotopy only affects points in $\widetilde{Z}$ near $\widetilde{F}_{all} \times [0,1] \subset \widetilde{C}_{all} \times [0,1]$ so it can be chosen to be the identity in $\left(\widetilde{C}_{all} - \eta(\widetilde{F}_{all})\right) \times [0,1]$. Thus $\widetilde{Z}$ is diffeomorphic to the union

$$\widetilde{Z} \;\approx\; \left(\left(\widetilde{C}_0 \cup_{\widetilde{F}_{all}} \widetilde{C}_1\right) \times [0,1]\right) \bigcup \widetilde{C}_{all} \times [0,1], \tag{10}$$

where we glue a neighborhood of the surface $\widetilde{F}_{all} \times \{0\}$ in $\left(\widetilde{C}_0 \cup_{\widetilde{F}_{all}} \widetilde{C}_1\right) \times \{0\}$ with the product $\widetilde{F}_{all} \times [0,1]$ in $\widetilde{C}_{all} \times [0,1]$.

Recall that a connected compression body C can be built from its negative boundary by adding $l = \frac{1}{2}\left(\chi(\partial_- C) - \chi(\partial_+ C)\right)$ 1-handles to $\partial_- C \times \{1\} \subset \partial_- C \times [0,1]$. If $\partial_- C = \emptyset$, one must add $(l+1)$ 1-handles to a 3-ball (0-handle). Thus, if $\widetilde{F}_{all} \neq \emptyset$ then $\widetilde{Z}$ is obtained by attaching 1-handles to $\left(\widetilde{C}_0 \cup_{\widetilde{F}_{all}} \widetilde{C}_1\right) \times [0,1]$ along $\left(\widetilde{C}_0 \cup_{\widetilde{F}_{all}} \widetilde{C}_1\right) \times \{0\}$. If $\widetilde{F}_{all}$ is empty, then $\widetilde{C}_{all}$ is a handlebody, $\widetilde{C}_0$ and $\widetilde{C}_1$ are empty, and $\widetilde{Z}$ is a 4-dimensional handlebody.

We can safely conclude that

$$\widetilde{Z} \approx (\text{0-handle}) \cup \left((\widetilde{C}_0 \cup_{\widetilde{F}_{all}} \widetilde{C}_1) \times [0,1]\right) \cup (|\delta_{all}| \text{ 1-handles}). \tag{11}$$

Remark 3.2. Even though the 3-manifold $\widetilde{C}_0 \cup_{\widetilde{F}_{all}} \widetilde{C}_1$ might be disconnected[2], each component of $\left(\widetilde{C}_0 \cup_{\widetilde{F}_{all}} \widetilde{C}_1\right) \times [0,1]$ has connected 3-manifold boundary. Thus, up to diffeomorphism, each 1-handle in Equation 11 corresponds to a boundary connected sum between two components or with a copy of $S^1 \times B^3$.

Remark 3.3. Suppose that all of the components of $\partial_- \widetilde{C}_0$ and $\partial_- \widetilde{C}_1$ are surfaces with boundary. By construction of $\widetilde{\delta}^0$ and $\widetilde{\delta}^1$, one can show that $\widetilde{C}_0 \cup_{\widetilde{F}_{all}} \widetilde{C}_1$ is also a 3-dimensional handlebody. Therefore, both the standard piece $\widetilde{Z}$ and Z are 4-dimensional 1-handlebodies in this specific case. Classical relative trisections satisfy this condition.

The following lemma is a refinement of Equation 11.

Lemma 3.4. $\widetilde{Z}$ is diffeomorphic to a boundary connected sum of a 4-dimensional 1-handlebody with the boundary connected sum of the trivial bundles $F \times D^2$, where F runs through the components of the negative boundary of $\widetilde{C}$.

Proof. We use the notation described at the begining of the subsection. Remark 3.2 allows us to only look at the connected components of $\widetilde{C}_0 \cup_{\widetilde{F}_{all}} \widetilde{C}_1$, which are in correspondance with $|\widetilde{F}_{all}|$. We then suppose that $\widetilde{F}_{all}$ is a connected non-empty surface.

The fact that $\widetilde{C}_{all}$ is the common sub-compression body between $\widetilde{C}^0$ and $\widetilde{C}^1$ implies that there are no essential simple closed curves in $\widetilde{F}_{all}$ bounding disks in both $\widetilde{C}_0$ and $\widetilde{C}_1$. In particular, if both collections of curves $\widetilde{\delta}_i$ are non-empty, then the result of compressing $\widetilde{F}_{all}$ along $\widetilde{\delta}_0 \cup \widetilde{\delta}_1$ contains no sphere components, and the compression body $\widetilde{C} - int(\widetilde{C}_{all})$, determined by $\widetilde{\delta}_0 \cup \widetilde{\delta}_1$ in $\widetilde{F}_{all}$, has non-empty negative boundary. In other words, we do not need 3-dimensional 3-handles to build $\widetilde{C} - int(C_{all})$ using the loops $\widetilde{\delta}_0 \cup \widetilde{\delta}_1$.

Suppose that both $\widetilde{\delta}_0$ and $\widetilde{\delta}_1$ are non-empty. The observation above tells us that no 3-handles are needed to build each $\widetilde{C}_i$. Thus the 3-manifold $\widetilde{C}_0 \cup \widetilde{C}_1$ is built from $\widetilde{F}_{all} \times [0,1]$ by attaching 2-handles along $\widetilde{\delta}_i \times \{i\} \subset$

[2]In fact $\widetilde{C}_0 \cup_{\widetilde{F}_{all}} \widetilde{C}_1$ has as many components as $|\widetilde{F}_{all}|$.

$\widetilde{F}_{all} \times \{i\}$ for $i = 0, 1$. This implies that $\left(\widetilde{C}_0 \cup \widetilde{C}_1\right) \times [0,1]$ can be built from $\widetilde{F}_{all} \times D^2 \approx \widetilde{F}_{all} \times [0,1]^2$ by attaching 4-dimensional 2-handles along $\widetilde{\delta}_i \times \{(-1)^i\} \subset \widetilde{F}_{all} \times \{(-1)^i\}$ for $i = 0, 1$ with framing given by the fiber surface. Since $\widetilde{\delta}_0$ and δ_1 are disjoint in $\widetilde{F}_{all}$, we can isotope the attaching regions of the 2-handles in $\widetilde{F}_{all} \times S^1$ to lie in the same fiber $\widetilde{F}_{all} \times \{1\}$. Using the previous paragraph we get that $\left(\widetilde{C}_0 \cup \widetilde{C}_1\right) \times [0,1]$ is diffeomorphic to $\left(\widetilde{C} - int(\widetilde{C}_{all})\right) \times [0,1]$. Notice that the same conclusion holds if one of $\widetilde{\delta}_i$ is empty.

To end, recall that $\widehat{C} = \widetilde{C} - int(\widetilde{C}_{all})$ is a compression body satisfying $\partial_+\widehat{C} = \widetilde{C}_{all}$ and $\partial_-\widehat{C} = \partial_-\widetilde{C}$. If $\partial_-\widehat{C}$ is empty, then $\widehat{C}$ is a handlebody and $\widetilde{Z} \approx \widehat{C} \times [0,1]$ is a 1-handlebody. On the other hand, if $\partial_-\widehat{C} \neq \emptyset$ then $\widehat{C}$ is built from $\left(\partial_-\widehat{C}\right) \times [0,1]$ by attaching 1-handles along $\left(\partial_-\widehat{C}\right) \times \{1\}$ and $\widetilde{Z}$ has the right diffeomorphism class. □

In order to build a standard 4-dimensional piece for a $\star$-trisection, we remove boundary parallel disks from the 4-manifold $\widetilde{Z}$. We want such disks to be defined solely by their boundary. This is the case when $\widetilde{Z}$ is a 4-ball [4] or a 1-handlebody [24]. The following technical lemma proves uniqueness for any $\widetilde{Z}$.

Lemma 3.5. Let $\widetilde{Z}$ as above, and let L be an unlink in $\partial\widetilde{Z}$. Up to isotopy fixing L, the unlink L bounds a unique collection of simultaneously boundary parallel disks in $\widetilde{Z}$.

Proof. The argument in the third paragraph of the proof of Lemma 8 of [24] proves the following statement: "Suppose A_1 and A_2 are 4-manifolds with connected boundary satisfying (1) A_i has unique trivial disks (up to isotopy relative their boundary), and (2) any embedded sphere in ∂A_i bounds a properly embedded 3-ball in A_i. Then $A_1 \natural A_2$ has unique trivial disks." Also in Lemma 8 of [24] is proven that 1-handlebodies satisfy properties (1) and (2). Hence, using the decomposition of Lemma 3.4, it is enough to check uniqueness of trivial disks for $F \times D^2$ where F is a connected closed surface of positive genus.

Let $F \neq S^2$ be a closed surface and let L be an unlink in $F \times S^1$. Suppose D and D' are two collections of properly embedded trivial disks in $F \times D^2$ with boundary equal to L. We want to show that they are isotopic relative to L. There exist a collection of disks D_* (resp. D'_*) in $F \times S^1$ isotopic to D (resp. D') via an isotopy fixing L. Perturb D_* and D'_* to intersect transversely (away from L) in a finite set of loops. Suppose $int(D_*) \cap int(D'_*) \neq \emptyset$.

Let $E \subset D_*$ be a disk with interior disjoint from D'_* and boundary a loop in $int(D_*) \cap int(D'_*)$. Let E' be the disk in D'_* with same boundary as E. Since $F \times S^1$ is irreducible, the embedded 2-sphere $E \cup E'$ bounds a 3-ball $B \subset F \times S^1$. Push the interior of B into $int(F \times D^2)$ to make it disjoint from D_* and D'_*, we can do this since $D_* \cup D'_*$ lies in $F \times S^1$. Isotope E' through B to remove the intersection loop $E \cap E' \subset int(D_*) \cap int(D'_*)$. We can perform this type of isotopy until $int(D_*) \cap int(D'_*) = \emptyset$. Again, the sphere $D_* \cup D'_*$ bounds a collection of 3-balls in $F \times S^1$ which we can use (as before) to isotope D_* onto D'_* as desired. □

3.2. Construction 2

Recall that a 3-dimensional compression body C can be built from its positive boundary F by attaching 2-handles along $F \times \{1\} \subset F \times [0,1]$ and 3-handles along the resulting spherical components. Thus $C \times [0,1]$ is obtained from $F \times [0,1]^2$ by attaching 4-dimensional 2-handles along loops in $F \times \{1\} \times \{1/2\}$ with framing given by the interval direction, and 4-dimensional 3-handles along the spheres obtained by compressing $F \times \{1\} \times \{1/2\}$ by the 2-handles.

Equation 9 of the previous subsection implies that $\widetilde{Z}$ can be built from $\widetilde{C}_{all} \times [0,1]$ by attaching 4-dimensional 2-handles along the loops $\widetilde{\delta}_0 \times \{1/4\} \subset \widetilde{F}_{all} \times \{1/4\}$ and $\widetilde{\delta}_1 \times \{3/4\} \subset \widetilde{F}_{all} \times \{3/4\}$ with framing given by the surface, and attaching 4-dimensional 3-handles along any 2-sphere obtained from compressing $\widetilde{F}_{all} \times \{1/4 + i/2\}$ along $\widetilde{\delta}_i \times \{1/4 + i/2\}$.

Suppose $\widetilde{F}_{all}$ is non-empty. We can build $\widetilde{C}_{all} \times [0,1]$ as above using the surface F_{k,b_0}, the curves $\widetilde{\delta}_{all}$, and no 3-handles. Furthermore, we can 'double' the 2-handles at the expense of adding 4-dimensional 3-handles as follows

$$\widetilde{C}_{all} \times [0,1] \approx F_{k,b_0} \times [0,1]^2 \cup \Big(\text{2-handles } \widetilde{\delta}_{all} \times \{1\} \times \{1/4, 3/4\}\Big) \cup (\text{3-handles})\,. \tag{12}$$

The core 2-spheres of the 3-handles in the previous equation are built by connecting the core disks of the 2-handles $\widetilde{\delta}_{all} \times \{1\} \times \{1/4, 3/4\}$ with the annuli $\widetilde{\delta}_{all} \times \{1\} \times [1/4, 3/4]$. For $i = 0, 1$, $F_{k,b_0} \times \{1\} \times \{1/4 + i/2\}$ compresses to a copy of $\widetilde{F}_{all}$. We can then glue copies of $\widetilde{C}_i \times [0,1]$ to $\widetilde{C}_{all} \times [0,1]$ in the form of 4-dimensional 2-handles and 3-handles as in the previous paragraph.

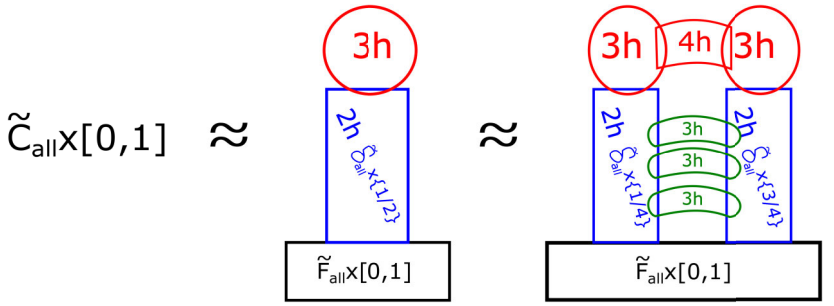

Figure 8: A schematic of $\widetilde{C}_{all} \times [0,1]$ after 'doubling' its 2-handles and 3-handle. In this paper we will normally find $\star$-trisections with $\widetilde{F}_{all} \neq \emptyset$. In such cases, we don't add the 3-handles and 4-handle in red in the figure and obtain the description in Equation 12.

Therefore, via Equation 9 we can conclude that $\widetilde{Z}$ is diffeomorphic to

$$F_{k,b_0} \times [0,1]^2 \cup \Big(\text{2-handles } \widetilde{\delta}^0 \times \{1\} \times \{1/4\} \text{ and } \widetilde{\delta}^1 \times \{1\} \times \{3/4\}\Big) \cup (\text{3-handles}), \tag{13}$$

where the 3-handles are attached along the sphere components obtained from compressing $F_{k,b_0} \times \{1\} \times \{1/4 + i\}$ along $\widetilde{\delta}^i \times \{1\} \times \{1/4 + i/2\}$, and the spheres built from the common curves in $\widetilde{\delta}_{all}$.

Remark 3.6. If $\widetilde{F}_{all} = \emptyset$, in order to build $\widetilde{C}_{all}$ you must add one final 3-dimensional 3-handle after attaching 2-handles to $F_{k,b_0} \times [0,1]$ along $\widetilde{\delta}_{all} \times \{1\}$. This final 3-handle becomes a 4-dimensional 3-handle when forming the product $\widetilde{C}_{all} \times [0,1]$ (see Figure 8), and can be 'doubled' at the expense of adding one 4-dimensional 4-handle (in the form of a 3-4-cancelling pair). In this situation, $\widetilde{C}_0$ and $\widetilde{C}_1$ are both empty, $F_{k,b_0} = F_k$ is a closed surface, and $\widetilde{C} = \widetilde{C}_{all}$ is a 3-dimensional handlebody. Hence $\widetilde{Z} = \widetilde{C}_{all} \times [0,1]$ is a 4-dimensional 1-handlebody with boundary admitting a Heegaard splitting of the form $\widetilde{C}_{all} \cup_{F_k} \widetilde{C}_{all}$. The resulting model of $\widetilde{Z}$ is the standard 4-dimensional piece of a 'classic' trisection of a closed, connected 4-manifold.

3.3. The unlink U and the standard piece Z

We are ready to discuss the 4-manifold Z in detail. We keep using the same notation as before.

Let $\widetilde{Y}$ be the 3-manifold given by the Heegaard splitting $\widetilde{Y} = \widetilde{C}^1 \cup_{F_{k,b_0}} \widetilde{C}^0$, and let $U \subset \widetilde{Y}$ be an unlink of unknots. $\widetilde{Y}$ embeds into $\partial\widetilde{Z}$ as

$$\widetilde{Y} \approx \left(\widetilde{C}^0 \times \{0\}\right) \cup (F_{k,b_0} \times [0,1]) \cup \left(\widetilde{C}^1 \times \{1\}\right) \subset \partial\widetilde{Z}.$$

Lemma 3.5 states that $U \subset \partial\widetilde{Z}$ bounds a unique[3] collection of properly embedded disks $D \subset \widetilde{Z}$ that can be isotoped (fixing U) into embedded disks in $\partial\widetilde{Z}$. Define Z to be a copy of $\widetilde{Z}$ after removing an open neighborhood of D. The facts that the disks are parallel to the boundary and $\widetilde{Y}$ is connected imply that Z is diffeomorphic to $\widetilde{Z} \natural \left(\natural_{|U|} S^1 \times B^3\right)$. In what follows, we will see that the 4-manifold Z can be built as in Subsection 3.2 using a new pair of compression bodies.

Isotope U in $\widetilde{Y}$ to be in bridge position with respect to the given Heegaard splitting. This means that for $i = 0, 1$ the intersection $U \cap \widetilde{C}^i$ consists of properly embedded arcs in $\widetilde{C}^i$ which can be projected to embedded arcs in $F_{k,b_0} = \partial_+\widetilde{C}^i$. We will refer to such projected arcs in F_{k,b_0} as shadows of $\widetilde{Y} \cap \widetilde{C}^i$. The number of arcs in $U \cap \widetilde{C}^0$ is called the number of bridges of U. Notice that $U \cap F_{k,b_0}$ is a set of $2|U \cap \widetilde{C}^0|$ points.

Let Y be the complement of U in $\widetilde{Y}$ and $C^i := \widetilde{C}^i - \eta(U)$. The intersection $C^0 \cap C^1$ becomes a copy of F_{k,b_0} with $2|U \cap \widetilde{C}^0|$ open disks removed. Furthermore, each C^i is a compression body with positive boundary the surface $F_{k,b}$, where $b = b_0 + 2|U \cap \widetilde{C}^0|$; and $Y = C^0 \cup_{F_{k,b}} C^1$ is a Heegaard splitting.

Since U is an unlink of unknots, we can think of Y as the connected sum of $\widetilde{Y}$ with the complement of an unlink U' in S^3. Using Haken's lemma we can choose the connected sum sphere S to intersect $F_{k,b}$ in one loop. Thus the loops in $F_{k,b_0} \subset \widetilde{Y}$ bounding disks in $\widetilde{C}^i$ can be identified with loops in $F_{k,b}$ bounding disks in C^i on one side of such separating sphere. We can further use Haken's lemma to find pairwise disjoint spheres S_*, away from S, decomposing $S^3 - \eta(U')$ into a connected sum of complements of unknots in S^3 in bridge position, satisfying that each component of S_* intersects $F_{k,b}$ in one loop.

In conclusion, we can find sets of curves $\delta^i \subset F_{k,b}$ determining the compression body C^i so that the loops $\widetilde{\delta}^i$ and $(S_* \cap F_{k,b})$ are contained in δ^i. Define $\delta_{all} = \widetilde{\delta}_{all} \cup (S_* \cap F_{k,b})$. Observe that the curves in δ^i consist in the loops in $\widetilde{\delta}^i$, together with the new loops in $(S_* \cap F_{k,b})$ and loops obtained from the complement of each unknot component of U. The proof of the

[3]Up to isotopy relative to the boundary.

following lemma (Figure 9) shows us how complicated these new loops can be.

Lemma 3.7. The 4-manifold Z can be built as in Equation 13 with $F_{k,b}$ and the loops δ^0, δ^1 and δ_{all}. More precisely, Z is diffeomorphic to

$$F_{k,b} \times [0,1]^2 \cup \big(\text{2-handles } \delta^0 \times \{1\} \times \{1/4\} \text{ and } \delta^1 \times \{1\} \times \{3/4\}\big) \cup (\text{3-handles}), \tag{14}$$

where the 3-handles are attached along the sphere components obtained from compressing $F_{k,b} \times \{1\} \times \{1/4 + i\}$ along $\delta^i \times \{1\} \times \{1/4 + i/2\}$ for $i = 0, 1$, and the spheres built from the common curves in δ_{all}.

Proof. Suppose first that each component of U has bridge number one. Since U is an unlink, we can find a set of disks $D_* \subset Y$ bounded by U intersecting $F_{k,b}$ in a single arc per disk in D_*. The spheres S_* in Y can be chosen to be $\partial\eta(D_*)$. In this case, the curves determining the compression bodies are given by $\delta^i = \widetilde{\delta} \cup (S_* \cap F_{k,b})$. Using such curves, the right hand side of Equation 14 is diffeomorphic to $\widetilde{Z} \natural \left(\natural_{|U|} S^1 \times B^3\right) \approx Z$, which is what we want. One way to see this is to first note that if $c \subset \delta_{all}$ is a separating curve decomposing $F_{k,b}$ as $F_{k_1,b_1} \#_c F_{k_2,b_2}$, then the 4-manifold from the right hand side decomposes as a boundary connected sum of 4-manifolds built in the same way from the surfaces F_{k_j,b_j} $(j = 1, 2)$; and then check that the 4-manifold obtained from an annulus $F_{0,2}$ and $\delta^0 = \delta^1 = \delta_{all} = \emptyset$ is $S^1 \times B^3$.

We now proceed with the general case. First recall that any bridge position of an unlink of unknots in a 3-manifold is always perturbed. This result was proven for S^3 in [25], and for any 3-manifold in [16]. A perturbation is a local isotopy of a link in bridge position around the Heegaard surface shown in Figure 9. It increases the bridge number by one. Figure 9 describes how the complement of the link changes after a perturbation, and shows us how the δ^i sets increase by one loop. The main observation is that the 4-manifolds built from the right hand side of Equation 14 are diffeomorphic because the operation of removing two disks to $F_{k,b}$ and adding two curves (not in δ_{all}) corresponds to add two 4-dimensional 1-2-cancelling pairs of handles (See Figure 9).

Hence, for any bridge position of U in $\widetilde{Y}$, after fixing a set of spheres S_*, we can slide the curves of $\delta^i - \delta_{all}$ over the curves in δ^i until 'detecting' a pair of curves intersecting like in Figure 9. This pattern determines a perturbation of U which we undo to decrease the bridge number, without changing the resulting 4-manifold. We can repeat this procedure until each

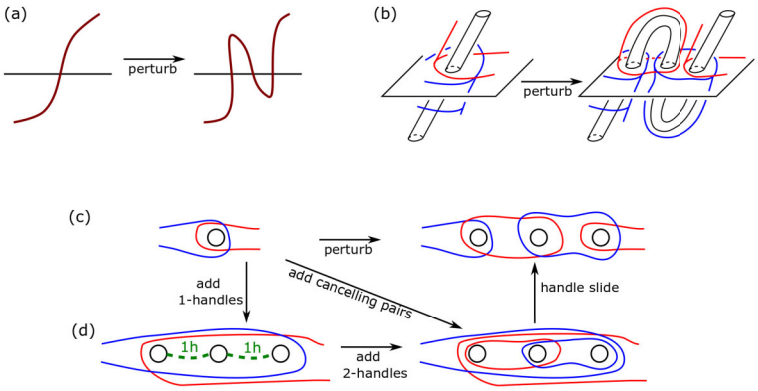

Figure 9: (a) An image of a perturbation of U around a point $U \cap F$. (b) How a perturbation changes the complement of U in both compression bodies. (c) A perturbation changes the collections of disks δ^i by adding a curve to each of them. (d) A perturbation changes the decomposition of the 4-dimensional piece by adding two 1-2-cancelling pairs of handles.

component of U has bridge number one, in which case the result is known. Therefore, for any bridge position of U, Equation 14 holds. □

Remark 3.8 (Stabilization). For an integer $g \geq k$, we can stabilize the Heegard splitting of $Y = C^0 \cup_{F_{k,b}} C^1$ $(g-k)$ times to obtain the decomposition $Y = Y^-_{C^0,C^1} \cup Y^+_{C^0,C^1}$. This changes the Heegaard diagram $(F_{k,b}; \delta^0, \delta^1)$ by connected sum with $(g-k)$ copies of the genus one diagram $(F_{1,0}; a_0, a_1)$, where a_0 and a_1 are loops intersecting once. We write the new diagram as $(\Sigma; \Delta^0, \Delta^1)$ where $\Sigma = F_{g,b}$ and $\Delta^i = \delta^i \cup \delta^i_{stab}$ and $(\delta^0_{stab}, \delta^1_{stab})$ correspond to the new dual loops. Note that stabilizations on the diagram correspond to adding two 1-2-cancelling pairs of handles to the 4-manifold built in Equation 14. Therefore, using Lemma 3.7 we conclude that Z is diffeomorphic to

$$\begin{aligned}(15)\quad & \Sigma \times [0,1]^2 \cup \big(\text{2-handles } \Delta^0 \times \{1\} \times \{1/4\} \text{ and } \Delta^1 \times \{1\} \times \{3/4\}\big) \\ & \qquad \cup \,(\text{3-handles})\,,\end{aligned}$$

where the 3-handles are attached along the sphere components obtained from compressing $\Sigma \times \{1\} \times \{1/4 + i\}$ along $\Delta^i \times \{1\} \times \{1/4 + i/2\}$ for $i = 0, 1$, and the spheres built by connecting the core disks of the 2-handles $\delta_{all} \times \{1\} \times \{1/4, 3/4\}$ with the annuli $\delta_{all} \times \{1\} \times [1/4, 3/4]$. Recall that we need to add extra 3-handles and 4-handles if $\widetilde{F}_{all}$ is empty (see Remark 3.6). Thus,

if both C^0 and C^1 are handlebodies (i.e., have empty negative boundary) then one of the boundary components of the resulting 4-manifold is a copy of S^4, which we cap-off uniquelly with one 4-handle. This last case occurs for classical trisections of closed 4-manifolds.

Denote by C_{all} the compression body built from $\Sigma \times [0,1]$ using the loops $\Delta_{all} = \Delta^0 \cap \Delta^1$ in Σ, and by F_{all} the negative boundary of C_{all}. By construction F_{all} is homeomorphic to a copy of $\widetilde{F}_{all}$, together with the disjoint union of planar surfaces (complements of the bridge spheres for each component of U). Denote by C_0 (resp. C_1) the compression body obtained from F_{all} and the curves in $\Delta_i = \Delta^i - \Delta_{all}$. Starting from Equation 15, we can undo the 'doubling' procedure in Subsection 3.2 and conclude that Z is diffeomorphic to the union

$$Z \approx C_0 \times [0,1/2] \bigcup_{F_{all}\times[0,1/2]} C_{all} \times [0,1] \bigcup_{F_{all}\times[1/2,1]} C_1 \times [1/2,1]. \tag{16}$$

Moreover, using Figure 4, we can check that Z is diffeomorphic to

$$Z \approx Y^-_{C^0,C^1} \times [0,1/2] \bigcup_{C_{all}\times\{1/2\}} Y^+_{C^0,C^1} \times [1/2,1]. \tag{17}$$

From here, we can perform the isotopy described in Subsection 3.1 and conclude that Z is diffeomorphic to the union

$$Z \approx ((C_0 \cup_{F_{all}} C_1) \times [0,1]) \bigcup C_{all} \times [0,1], \tag{18}$$

where we glue a neighborhood of the surface $F_{all} \times \{0\}$ in $(C_0 \cup_{F_{all}} C_1) \times \{0\}$ with the product $F_{all} \times [0,1]$ in $C_{all} \times [0,1]$.

Remark 3.9 (Diagrammatics). The previous equations show us several equivalent ways of building the standard 4-manifold piece Z using the compression bodies C^0, C^1 and C_{all} which are determined by the tuple $(\Sigma; \Delta^0, \Delta^1, \Delta_{all})$ up to isotopies and handle slides. The combinatorics of the loops Δ^0 and Δ^1 in Σ is summarized in Figure 10. The curves on each set Δ^i are pairwise disjoint and the sets decompose as $\Delta^i = \delta^i_{stab} \cup \Delta_{all} \cup \Delta_i$. The curves in δ^0_{stab} and δ^1_{stab} are in bijective correspondence and only the paired loops intersect in exactly one point while the rest are pairwise disjoint. The curves in Δ_{all} are in both Δ^0 and Δ^1 and are pairwise disjoint. There are two types of families of loops in $\Delta_0 \cup \Delta_1$: the fist type is formed of non-isotopic pairwise disjoint loops (identified with loops in $\widetilde{\delta}_i \subset F_{k,b_0}$); the loops in the second type form Heegaard splittings of the complement of an

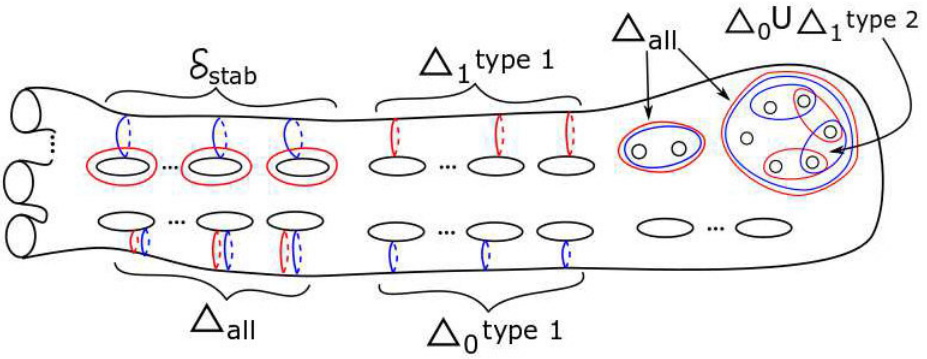

Figure 10: The combinatorics of the tuple $(\Sigma; \Delta^0, \Delta^1, \Delta_{all})$. For this example, observe that U has two components, one of which has bridge number one and the other bridge number three.

unknot in bridge position (obtained from the trivial arcs of each component of U).

3.4. The boundary of Z

Let C be a compression body built from $F \times [0,1]$ by attaching some 3-dimensional 2-handles along $F \times \{1\}$. Recall that the boundary of C is given by copies of its positive boundary ($F \times \{0\}$) and its negative boundary (the non-spherical components of $F \times \{1\}$ after compression), connected by annuli of the form $\partial_0 C := (\partial F) \times [0,1]$.

Let $B := (\partial F) \times \{1/2\} \times \{1/2\}$ be the core of the solid torus $(\partial_0 C) \times [0,1]$ inside $\partial(C \times [0,1])$. The 3-manifold $\partial(C \times [0,1]) - \eta(B)$ can be built by taking two copies of C and gluing their negative (and positive) boundaries together using the identity map. Such splitting induces a circular handle decomposition of $\partial(C \times [0,1])$ with binding B, built from $F \times [0,1]$ by attaching 2-handles on both sides $F \times \{0,1\}$ and identifying the resulting non-spherical components[4] (see Figure 11). Using Equation 17, we can glue the circular handle decompositions for $\partial(Y^- \times [0,1/2])$ and $\partial(Y^+ \times [1/2,1])$ together along $C_{all} \times \{1/2\}$ to find a circular handle decomposition of the

[4]Recall we always attach 3-handles along the new sphere components. In particular, if C is a handlebody this contruction yields the classical handle decomposition of $\#S^1 \times S^2$ which we still think of circular.

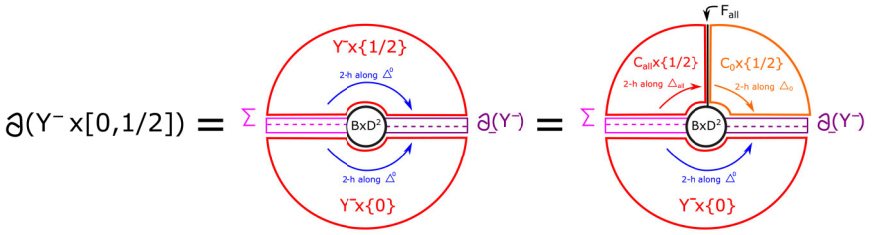

Figure 11: Circular handle decomposition on $\partial\left(Y^{-} \times [0,1/2]\right)$. We can further decompose one copy of Y^{-} as $C_{all} \cup_{F_{all}} C_0$.

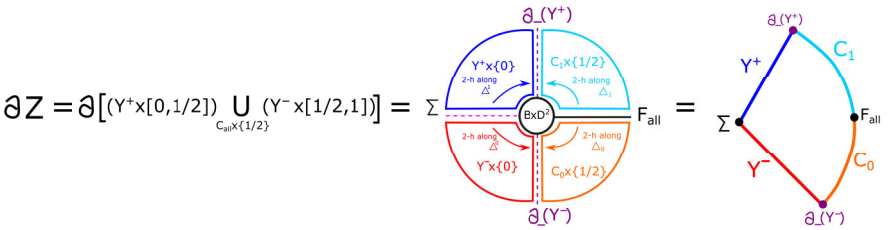

Figure 12: How to build ∂Z using the tuple $\left(\Sigma; \Delta^0, \Delta^1\right)$. Compare with right side of Figure 4.

boundary of a standard piece $Z(C^0, C^1, C_{all})$. We draw them in Figures 11 and 12.

Remark 3.10 (Boundary of X). In a $\star$-trisected 4-manifold $X = X_1 \cup X_2 \cup X_3$, the pieces labeled $Y^{\pm}$ on the boundary of all standard pieces X_i are glued together. This implies that $X_i \cap \partial X$, away from $\eta(B)$, is of the form $C_0 \cup_{F_{all}} C_1$ (see Figure 12) which is the disjoint union of Heegaard splittings with Heegaard surfaces being the components of F_{all}. Thus the boundary of X admits a circular handle decomposition with binding the boundary of the trisection surface $B = \partial\Sigma$. The decomposition on $\partial X - \eta(B)$ can be obtained by taking copies of the 3-manifolds $C_0 \cup_{F_{all}} C_1$ obtained from each X_i and gluing $\partial_{-} C_0$ from X_i with $\partial_{-} C_1$ from X_{i+1} as in Figure 5.

4. Trisection diagrams

In this section we will describe the diagrammatics of $\star$-trisections. We will compare our notion of trisection diagrams with the existent literature. We

end this section by discussing a diagramatic operation on $\star$-trisections with boundary called poking.

Let $X = X_1 \cup X_2 \cup X_3$ be a $\star$-trisected 4-manifold. The trisection surface $\Sigma = X_1 \cap X_2 \cap X_3$ is a connected orientable surface of genus g and $b \geq 0$ boundary components. The pairwise intersection $X_i \cap X_j$ is a compression body with positive boundary the surface Σ, denote the compresion bodies by $H_\alpha = X_1 \cap X_3$, $H_\beta = X_2 \cap X_3$ and $H_\gamma = X_1 \cap X_2$. By definition, the 4-manifold piece X_1 is diffeomorphic to the 4-manifold $Z(H_\gamma, H_\alpha, H_{\gamma\cap\alpha})$ for a given common subcompression body $H_{\gamma\cap\alpha}$ of H_γ and H_α. Let $\Delta_{\gamma\cap\alpha}$ be loops in Σ determining the compression body $H_{\gamma,\alpha}$. We define $H_{\alpha\cap\beta}$, $\Delta_{\alpha\cap\beta}$, $H_{\beta\cap\gamma}$ and $\Delta_{\beta\cap\gamma}$ in a similar way. Let α, β and γ be loops in Σ determining the compression bodies H_α, H_β and H_γ, respectively.

Due to Equation 15, we can use the tuple $(\Sigma; \alpha, \beta, \gamma; \Delta_{\gamma\cap\alpha}, \Delta_{\alpha\cap\beta}, \Delta_{\beta\cap\gamma})$ to build the 4-manifold X as follows: Let $p_\alpha^\pm$, $p_\beta^\pm$, $p_\gamma^\pm$ be six distinct points in the unit circle as in Figure 13. Start with $\Sigma \times D^2$ and glue copies of collars of the compresion bodies[5] $H_\varepsilon \times [p_\varepsilon^-, p_\varepsilon^+]$ along the arcs $[p_\varepsilon^-, p_\varepsilon^+] \times \Sigma$ for $\varepsilon \in \{\alpha, \beta, \gamma\}$. For each pair $(\varepsilon, \mu) \in \{(\gamma, \alpha), (\alpha, \beta), (\beta, \gamma)\}$, the compression bodies $H_\varepsilon \times \{p_\varepsilon^\pm\}$ are contained in the boundary of the resulting 4-manifold, and the 'common' curves $\Delta_{\varepsilon\cap\mu} \times \{p_\varepsilon^-, p_\mu^+\}$ bound disks on them. Attach 4-dimensional 3-handles with core spheres given by connecting such disks with the annuli $\Delta_{\varepsilon\cap\mu} \times [p_\varepsilon^-, p_\mu^+]$. If one of the common compression bodies has empty negative boundary (see Remark 3.6), say $\partial_- H_{\alpha\cap\beta} = \emptyset$, after adding the 3-handles, the new boundary will have a component homeomorphic to S^3 in the interval $[p_\alpha^-, p_\beta^+]$. In such case, we attach a 4-dimensional 4-handle to cap-off the S^3 component. The end result is our trisected 4-manifold X.

Remark 4.1 (Diagrammatics). We will refer to the data

$$(\Sigma; \alpha, \beta, \gamma; \Delta_{\gamma\cap\alpha}, \Delta_{\alpha\cap\beta}, \Delta_{\beta\cap\gamma})$$

as a $\star$-trisection diagram. The curves of a given diagram can be modified via handle slides along curves of the same label, or via homeomorphisms of the surface Σ without changing the diffeomorphism class of the $\star$-trisected 4-manifold. The authors of this paper find the following interpretation of $\star$-trisection diagrams useful: A $\star$-trisection diagram is a tuple $(\Sigma; \alpha, \beta, \gamma)$ such that each pair $(\varepsilon, \mu) \in \{(\gamma, \alpha), (\alpha, \beta), (\beta, \gamma)\}$, after adding

[5]This is equivalent to add 4-dimensional 2-handles to $\Sigma \times D^2$ along $\varepsilon \times \{p_\varepsilon\}$ with framing given by the surface, and 3-handles along the sphere components obtained by compressing $\Sigma \times \{pt_\varepsilon\}$ for $\varepsilon \in \{\alpha, \beta, \gamma\}$.

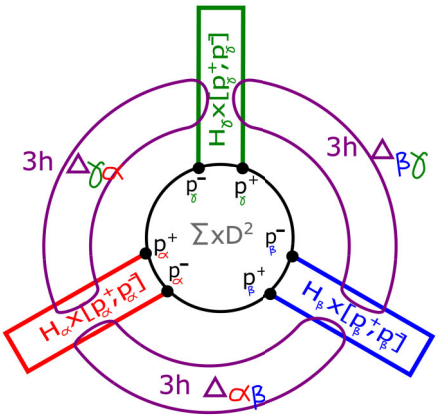

Figure 13: A schematic of how to build X from the tuple $(\Sigma; \alpha, \beta, \gamma; \Delta_{\gamma\cap\alpha}, \Delta_{\alpha\cap\beta}, \Delta_{\beta\cap\gamma})$. Compare this with Figure 8.

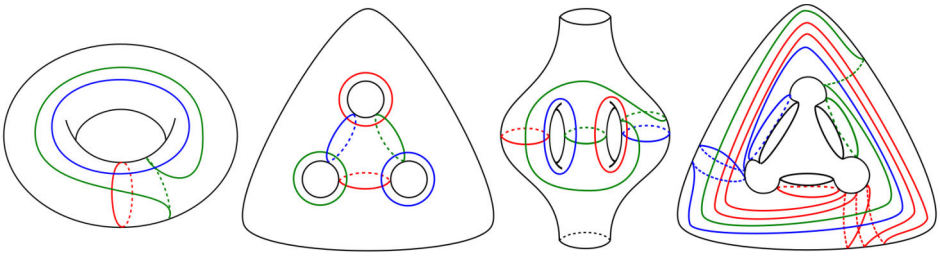

Figure 14: (left to right) A trisection of $\mathbb{CP}^2$, a relative trisection of the spin of $S^1 \times D^2$, a relative trisection of a disk bundle over S^2 with $e = -1$, a $\star$-trisection of $\mathbb{CP}^2 \setminus \eta(S^1)$.

some redundant curves to the ε, μ sets, is handle slide equivalent to a standard pair (Δ^0, Δ^1) from Remark 3.9 with $\Delta_{\varepsilon\cap\mu} = \Delta_{all}$. Figure 14 shows examples of various $\star$-trisection diagrams with empty common curves; i.e. $\Delta_{\gamma\cap\alpha} = \Delta_{\alpha\cap\beta} = \Delta_{\beta\cap\gamma} = \emptyset$. In Section 6 we will see why the rightmost figure is a $\star$-trisection diagram.

Remark 4.2 (Classic diagrams). For **classical** trisections, each pair of curves (ε, μ) in a relative trisection diagram is slide equivalent to a standard pair (Δ^0, Δ^1) diffeomorphic to the one in Figure 5 of [7]. In particular the Δ^i sets decompose as $\Delta^i = \Delta_{all} \cup \delta^i_{stab}$, making the information of the $\Delta_{\varepsilon\cap\mu}$ redundant. In this case the tuple $(\Sigma; \alpha, \beta, \gamma)$ is enough to build the

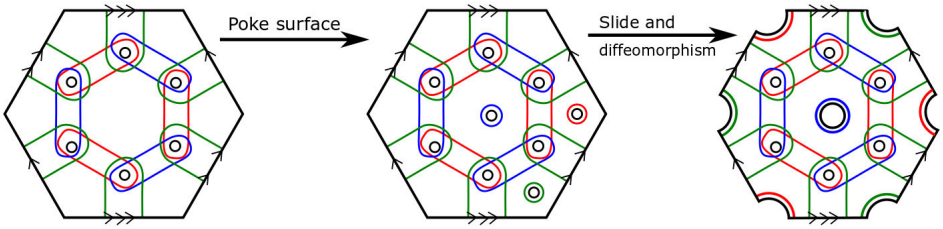

Figure 15: Example of how to poke a ⋆-trisection diagram.

4-manifold X. For general compression bodies H_ε and H_μ the choice of the common compression body $H_{\varepsilon\cap\mu}$ may not be unique, forcing us to record $\Delta_{\varepsilon\cap\mu}$ in the ⋆-trisection diagram. Fortunately, the choice of common curves will be easy to see for most of the ⋆-trisection diagrams that appear in this paper.

4.1. New relative diagrams from old

Let $\mathcal{D} = (\Sigma; \alpha, \beta, \gamma; \Delta_{\gamma\cap\alpha}, \Delta_{\alpha\cap\beta}, \Delta_{\beta\cap\gamma})$ be a ⋆-relative trisection diagram (see Remark 4.1) for a 4-manifold X with non-empty boundary. Let $p_\alpha, p_\beta, p_\gamma \subset \Sigma - (\alpha \cup \beta \cup \gamma)$ be three finite collections of points. Define $\mathcal{D}' = (\Sigma'; \alpha', \beta', \gamma'; \Delta_{\gamma\cap\alpha}, \Delta_{\alpha\cap\beta}, \Delta_{\beta\cap\gamma})$ be a new tuple given by $\Sigma' = \Sigma - \mathring{\eta}(p_\alpha \cup p_\beta \cup p_\gamma)$ and $\varepsilon' = \varepsilon \cup \partial\eta(\varepsilon)$ for $\varepsilon = \alpha, \beta, \gamma$. Using Equation 15 one can show that if $\mathcal{D}'$ is a ⋆-trisection diagram, then it is a diagram for X. We will refer to the operation of replacing $\mathcal{D}$ by $\mathcal{D}'$ by **poking**.

Poking a ⋆-trisection diagram adds new boundary components to the trisection surface and to the negative boundaries of the compression bodies C_α, C_β and C_γ. This operation comes handy when gluing ⋆-trisections. One condition for two ⋆-trisections to be able to be glued along their boundaries is that the surfaces $\partial_- C_\varepsilon$ $(\varepsilon = \alpha, \beta, \gamma)$ have all non-empty boundary. Figure 15 shows an example of how to poke a ⋆-trisection diagram in order to satisfy this condition.

In practice, one can poke a diagram by drawing one pair of curves, say (α, β), into standard position (Δ^0, Δ^1), and then pick the poking points $p_\gamma \subset \Sigma - (\alpha \cup \beta \cup \gamma)$ whenever needed. The location of the points in p_γ with respect to the curves in γ is irrelevant since we think of the curves in a diagram defined up-to handle slides and we can always slide $\partial\eta(p_\gamma)$ over γ as required.

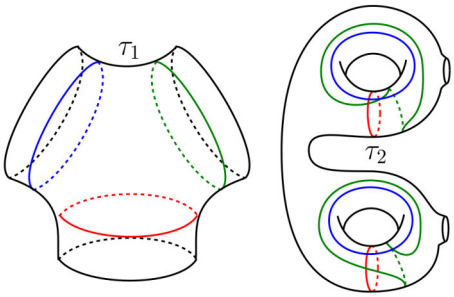

Figure 16: Two relative trisection diagram for $S^2 \times D^2$.

Remark 4.3 (Relative double twists). If we can pick points $|p_\alpha| = |p_\beta| = |p_\gamma| = 1$ so that all lie in the same component of $\Sigma - (\alpha \cup \beta \cup \gamma)$, poking corresponds to connect sum the given $\star$-trisection diagram with the diagram τ_1 in Figure 16. In this case, one could also connect sum the diagram τ_2 instead and still obtain a $\star$-trisection of the same 4-manifold. The new diagram will change the circular handle decomposition in the boundary by taking a solid torus neighborhood of a regular circle fiber and replacing it with the Seifert fibered space $S(0, 1; +1, -1)$. For relative trisection diagrams, the new monodromy is given by composing one positive and one negative Dehn twist along the two new boundary components, respectively (see Section 3.1 of [10]). The operation of connect summing (when possible) a relative trisection diagram with τ_2 is exactly the relative double twist move defined by Castro, Islambouli, Miller and Tomova in [8]. Using this move, the authors were able to show that any two relative trisections for the same 4-manifold with connected boundary and non-closed trisection surface ($b > 0$) are related by sequence of ambient isotopies, stabilizations, relative stabilizations, relative double twists, and the inverses of these moves.

5. Pasting $\star$-trisections

Motivated by the work of Castro and Ozbagci [6, 9], we want to describe a method to paste two compatible $\star$-trisections along their boundaries. The main technical observation that makes Theorem 5.1 work is that when we paste two standard pieces $Z(C^0, C^1, C_{all})$ along some connected components of $C_0 \cup_{F_{all}} C_1$, the resulting 4-manifold is also a standard piece whenever all the glued surfaces in F_{all} have boundary. The interested reader might note

that our proof follows the same outline that the one of Theorem 2 of [6] applied to the setting of $\star$-trisections.

We first review the circular handle decomposition on a $\star$-trisected 4-manifold. Let $X = X_1 \cup X_2 \cup X_3$ be a 4-manifold with a fixed $\star$-trisection. Let $B := \partial\Sigma$ be the boundary of the trisection surface embedded as a link in ∂X; B might be empty. Observe that $\partial X - \eta(B)$ decomposes as the union of three 3-manifolds, one per 4-dimensional piece. Remark 3.10 states that for each $i = 1, 2, 3$, the 3-manifold $X_i \cap (\partial X - \eta(B))$ admits a Heegaard splitting of the form $C_{(i),0} \cup_{F_{(i),all}} C_{(i),1}$. The compression bodies in this decomposition are obtained from the data in the identification $X_i \approx Z(C^0_{(i)}, C^1_{(i)}, C_{(i),all})$ and have as many connected components as $F_{(i),all}$ (see Remark 3.8 for more details).

Theorem 5.1 (Pasting lemma for $\star$-relative trisections). Let $W = W_1 \cup W_2 \cup W_3$ and $W' = W'_1 \cup W'_2 \cup W'_3$ be two $\star$-trisected 4-manifolds with non-empty boundary. Let $M \subset W$ and $M' \subset W'$ be closed 3-manifolds of the boundary of each 4-manifold. Let $f : M \to M'$ be a homeomorphism satisfying $f(W_i \cap M) = W'_i \cap M'$ and preserving the Heegaard decompositions on $W_i \cap M$ and $W'_i \cap M'$ induced by the trisections for all i. Suppose that each component of the surfaces $W_i \cap W_j \cap M$ and $W'_i \cap W'_j \cap M'$ has boundary for all $i \neq j$. Then $X = W \cup_f W'$ admits a $\star$-trisection with pieces given by $W_i \cup_f W'_i$ $(i = 1, 2, 3)$, and $\star$-trisection surface the result of gluing the trisection surfaces of W and W' along their boundary components intersecting with M and M', respectively.

Proof. Let $X_i = W_i \cup_f W'_i$. We will show that $X = X_1 \cup X_2 \cup X_3$ is a $\star$-trisection.

We will first focus on the pairwise intersection $X_i \cap X_j$. Fix $i \neq j$ and let $C = W_i \cap W_j$ and $C' = W'_i \cap W'_j$. By definition C and C' are compression bodies with positive boundary the connected $\star$-trisection surfaces Σ and Σ', respectively. Let $P_M = \partial_- C \cap M$ and $P_{M'} = f(P_M) = \partial_- C' \cap M'$ be the negative boundary components of C and C' lying inside the gluing regions M and M'. By assumption each component of P_M and $P_{M'}$ is a surface with boundary. This implies that $H = C \cup_f C'$ is also a compression body with positive boundary $\widetilde{\Sigma} = \Sigma \cup_f \Sigma'$. In particular, the triple intersection $X_1 \cap X_2 \cap X_3$ is a copy of $\widetilde{\Sigma}$. Let $\varepsilon \subset \Sigma$ and $\varepsilon' \subset \Sigma'$ be loops determining C and C'. Let $a \subset P_M$ be pairwise disjoint properly embedded arcs which cut P_M into disks and let $a' = f(a)$ be the corresponding arcs in $P_{M'}$. We can think of the arcs in a (resp. a') as subsets of Σ (resp. Σ'), disjoint from ε

(resp. ε'). The curves in $\widetilde{\Sigma} = \Sigma \cup_f \Sigma'$ determining H are given by $\varepsilon \cup \varepsilon'$ and the glued arcs $a \cup_f a'$.

We now show that each piece X_i is diffeomorphic to a standard piece. Fix $i \in \{1, 2, 3\}$, by definition $W_i \approx Z(C^0, C^1, C_{all})$ and $W_i' \approx Z(C'^0, C'^1, C'_{all})$ for some compression bodies. We use the notation of Remark 3.9; i.e., C^0 and C^1 are determined by essential loops $\Delta^0, \Delta^1 \subset \Sigma$, and the common curves $\Delta_{all} = \Delta^0 \cap \Delta^1$ determine the C_{all}. Let F_{all} be the negative boundary of C_{all}. For $j = 0, 1$ let $C_j = C^j - int(C_{all})$ be the compression body with positive boundary the surface F_{all}, and let P_j be the negative boundary of C_j. Recall that, due to Remark 3.10, $W_i \cap \partial W$ contains a copy of $C_0 \cup_{F_{all}} C_1$.

If F_{all} is disconnected, we can pick $\Delta_{all} \subset \Sigma$ having separating simple closed curves. Each such curve decomposes the diagram $(\Sigma; \Delta^1, \Delta^0, \Delta_{all})$ as a connected sum of standard diagrams in lower genus surfaces. This decomposes W_i into a boundary connected sum of the corresponding standard 4-manifolds. The same argument holds for W_i'. Hence, it is enough to check that $W_i \cup_f W_i'$ is a standard piece when F_{all} and F'_{all} are connected surfaces.

Suppose F_{all} is a connected surface. In particular, the curves in $\Delta_{all} \subset \Sigma$ do not separate the surface and C_{all} is built from $F_{all} \times [0, 1]$ by attaching $|\Delta_{all}|$ 1-handles[6] along $F_{all} \times \{1\}$. Then, using Equation 18 we conclude that W_i is diffeomorphic to the result of adding $|\Delta_{all}|$ 1-handles to $(C_0 \cup_{F_{all}} C_1) \times [0, 1]$. Since F_{all} is connected, Remark 3.2 explains that the location of the feet of the 1-handles is not necessary. Furthermore, since $(\Sigma; \Delta^0, \Delta^1, \Delta_{all})$ is a standard pair and F_{all} is connected, it follows that $\Delta_0 \cup \Delta_1$ only has curves of one type (see Remark 3.9). In any case, we get that $(C_0 \cup_{F_{all}} C_1) \times [0, 1])$ is a 1-handlebody of genus N. Here $N = \big(1 - \chi(F_{all}) - |\Delta_0| - |\Delta_1| - 2|\delta^0_{stab}|\big)$ if $\Delta_0 \cup \Delta_1$ is of type 1 or $N = 1$ if type 2. One can see this by building W_i like in Equation 15 and noticing that each circle in $\Delta_0 \cup \Delta_1$ cancels a 1-handles from the 1-handlebody $F_{all} \times [0, 1]^2$ (recall F_{all} has boundary). On the other hand, to build X_i we must glue $(C_0 \cup_{F_{all}} C_1) \times [0, 1]$ and $(C_0' \cup_{F'_{all}} C_1') \times [0, 1]$ using $f \times \{1\}$, and then add copies of $C_{all} \times [0, 1]$ and $C'_{all} \times [0, 1]$ as in Equation 18 (see right side of Figure 7). Therefore, $X_i = W_i \cup_f W_i'$ is a 1-handlebody of genus $K = |\Delta_{all}| + |\Delta'_{all}| + N$.

To end, observe that the boundary of $X_i = W_i \cup_f W_i'$ has a decomposition of the form $H^0 \cup_{\widetilde{\Sigma}} H^1$ where $H^j = (C^j \cup_f C'^j)$. In particular, both H^0 and H^1 are handlebodies and this is a Heegaard splitting for $\partial X_i = \#_K S^1 \times S^2$. Waldhausen's Theorem [26] implies that this splitting is a $g(\widetilde{\Sigma}) - K$ times stabilization of the standard genus K Heegaard splitting. We can take this standard splitting to be H_{all} and conclude that X_i

[6]No 3-handles are needed in this case since we are assuming F_{all} is non empty.

is diffeomorphic to the standard piece $Z(H^1, H^0, H_{all})$. This finishes the proof. □

Remark 5.2 (The diagrammatics). Take two $\star$-trisected 4-manifolds W, W' with a diffeomorphism $f : M \to M'$ between closed submanifolds of their boundaries respecting the handle respective handle decompositions. Suppose that all components of $W_i \cap W_j \cap M$ have non-empty boundary. Let $(\Sigma; \alpha, \beta, \gamma; \Delta_{\gamma\cap\alpha}, \Delta_{\alpha\cap\beta}, \Delta_{\beta\cap\gamma})$ be a $\star$-trisection diagram for W (resp. W'). Using Lemma 5.1, we get a $\star$-trisection diagram $(\widetilde{\Sigma}; \widetilde{\alpha}, \widetilde{\beta}, \widetilde{\gamma}; \Delta_{\widetilde{\gamma}\cap\widetilde{\alpha}}, \Delta_{\widetilde{\alpha}\cap\widetilde{\beta}}, \Delta_{\widetilde{\beta}\cap\widetilde{\gamma}})$ for $X = W \cup_f W'$ with trisection surface $\widetilde{\Sigma} = \Sigma \cup_f \Sigma'$. For $\widetilde{\varepsilon} = \widetilde{\alpha}, \widetilde{\beta}, \widetilde{\gamma}$, the curves in the compression body $H_{\widetilde{\varepsilon}}$ are given by:

1) Loops in $\varepsilon \subset \Sigma$ and $\varepsilon' \subset \Sigma'$.
2) Disks obtained from pairwise disjoint arcs filling the compressed page P_ε, glued along their boundaries to their images on $P_{\varepsilon'}$ under f.

In the proof of Lemma 5.1 we showed that the curves in $(\widetilde{\varepsilon}, \widetilde{\mu})$ obtained from the second item above are slide equivalent to a collection of isotopic curves and curves intersecting in one point (coming from stabilizations). Thus the curves in $\Delta_{\widetilde{\varepsilon}\cap\widetilde{\mu}}$ are given by the curves in $\Delta_{\varepsilon\cap\mu} \cup \Delta_{\varepsilon'\cap\mu'}$, together with this new parallel curves.

Since relative trisections with non-empty binding ($b > 0$) satisfy the conditions of Lemma 5.1, our result extends the gluing theorems of [6] and [9]. In this case ($b > 0$), the monodromy algorithm of [5] is helpful to find the image of the filling arcs under f. In general, in order to glue two $\star$-trisections with Theorem 5.1, one might need to poke the given diagrams (see Subsection 4.1) enough times to ensure that every connected component $\partial_-(W_i \cap W_j)$ is a surface with boundary. In particular, for relative trisections with $b = 0$, it is sufficient to poke the trisection surface three times.

Corollary 5.3 (Pasting lemma for relative trisections with empty binding). Let $W = W_1 \cup W_2 \cup W_3$ and $W' = W'_1 \cup W'_2 \cup W'_3$ be two trisected 4-manifolds with non-empty connected boundary and **closed** trisection surfaces Σ and Σ', respectively. Let P and P' be the pages of the fibration over S^1 on ∂W and $\partial W'$ induced by the trisections, respectively. Let $f : \partial W \to \partial W'$ be a homeomorphism between the boundaries respecting the pages; i.e., $f(P) = P'$. Then the glued closed 4-manifold $X = W \cup_f W'$

admits a $(G;K)$-trisection where

$$G = g(\Sigma) + g(\Sigma') + 2 \text{ and } K_i = k_i + k_i' + 2g(P).$$

Here k_i denote the number of common curves in the trisection diagrams.

Remark 5.4 (Diagrammatics for relative trisections with empty binding). Suppose now that we are given two relative trisection diagrams with **closed trisection surface** for two 4-manifolds with connected boundary. Suppose that we are also given a homeomorphism $f : \partial W \to \partial W'$ between connected components of the boundaries preserving the pages of the open book decomposition. To build the trisection diagram for the union $W \cup_f W'$ we need to find three poking points $p_\alpha, p_\beta, p_\gamma \subset \Sigma - (\alpha \cup \beta \cup \gamma)$. These points can be thought as lying in a page P for the open book decomposition in ∂W. Thus we can take their image under f to be points in the page $P' \subset \partial W'$. Denote by $p'_\alpha, p'_\beta, p'_\gamma \subset \Sigma' - (\alpha' \cup \beta' \cup \gamma')$ the corresponding points in Σ'. It follows that these are also poking points and the two new trisection diagrams for W and W' (obtained by poking) satisfy the conditions of Lemma 5.1. Hence, $W \cup_f W'$ admits a trisection diagram $(\widetilde{\Sigma}; \widetilde{\alpha}, \widetilde{\beta}, \widetilde{\gamma})$ with trisection surface

$$\widetilde{\Sigma} = \left(\Sigma - \cup_\varepsilon \mathring{\eta}(\varepsilon)\right) \bigcup_{\partial\eta(\varepsilon)=\partial\eta(\varepsilon')} \left(\Sigma' - \cup_{\varepsilon'} \mathring{\eta}(\varepsilon')\right).$$

For $\widetilde{\varepsilon} = \widetilde{\alpha}, \widetilde{\beta}, \widetilde{\gamma}$, the curves in $\widetilde{\varepsilon}$ are given by:

1) Loops in $\varepsilon \subset \Sigma$ and $\varepsilon' \subset \Sigma'$.
2) Disks obtained from pairwise disjoint arcs filling the compressed page P_ε, glued along their boundaries to their images on $P_{\varepsilon'}$ under f.
3) The loop $\partial\eta(p_\varepsilon)$.

Example 5.5 (Sphere bundles over RP^2). During the last day of the 2019 Spring Trisectors Meeting at UGA, the pair of trisection diagrams of Figure 19 was discussed. Work of Gay and Meier in [15] shows that B is a Gluck twist of A along some embedded 2-sphere. We can use Theorem 5.1 to decompose the 4-manifolds A and B as the union of two 4-manifolds along glued along their boundary: $A = (S^2 \times D^2) \cup_f X$ and $B = (S^2 \times D^2) \cup_g X$. Remark 6.2 and Figure 23 show that X is the complement of a circle in $S^1 \times S^3$ representing twice the generator of first homology. We can think of

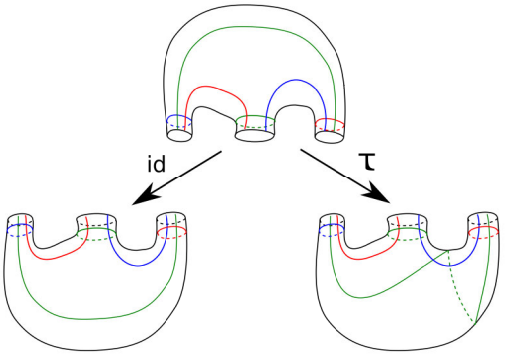

Figure 17: Two distinct ways of gluing a pair of thickened spheres. The map τ twists the S^2 fiber once while traversing the S^1 direction.

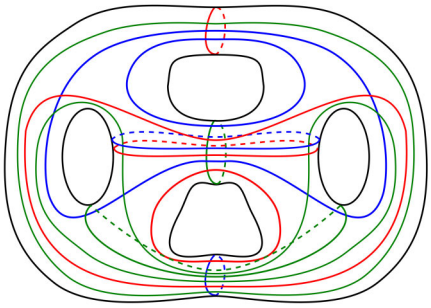

Figure 18: Trisection diagram for $T^2 \times S^2$. One can see two thrice punctured tori (left and right) corresponding to each copy of $T^2 \times D^2$.

this circle as the points $\{0\} \times \{\pm 1\}$ in $\{0\} \times S^1 \subset \{0\} \times S^3$ being rotated by π-radians when traversing in the S^1 direction. This way, X is the total space of a non-orientable bundle of 2-spheres over a Möbius band. Hence, A is the total space of S^2-bundle over RP^2 and B is a Gluck twist along a fiber.

6. The complement of a simple closed curve

Let X be a compact 4-manifold with $\star$-trisection $X = X_1 \cup X_2 \cup X_3$. Let Σ be the trisection surface and consider $c \subset X$ a simple closed curve in X. Since $\pi_1(\Sigma) \twoheadrightarrow \pi_1(X)$, the curve c is homotopic to an immersed curve $S^1 \looparrowright \Sigma$. Given an immersed curve as such, we are interested in finding a

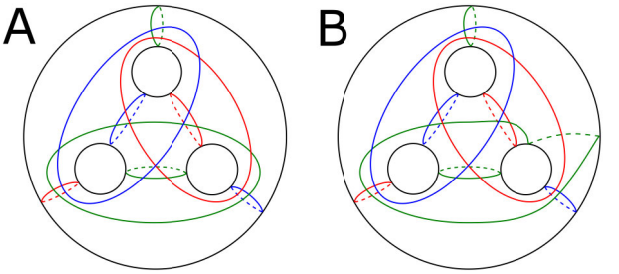

Figure 19: A pair of genus 3 trisection diagrams that differ by Gluck twist.

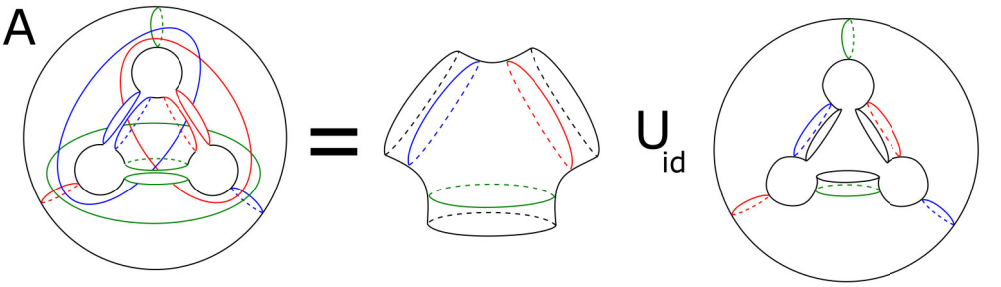

Figure 20: Decomposing A as $A = (S^2 \times D^2) \cup_f X$. Note that X is a trisection diagram for the complement of a circle in $S^1 \times S^3$ representing twice the generator of first homology. (see Section 6.1).

$\star$-trisection for $X - \eta(c)$. To accomplish this, we decompose the immersed curve into a union of embedded arcs, push the arcs into the handlebodies, and then remove the tubular neighborhood of each arc.

Definition 6.1. Given a $\star$-trisection $(\Sigma; \alpha_1, \alpha_2, \alpha_3)$, we say that an immersed curve $c \subset \Sigma$ is decomposed if c is the union of three collections of embedded arcs $c = a_1 \cup a_2 \cup a_3$ with the property that $a_1 \cap \alpha_1 = a_2 \cap \alpha_2 = a_3 \cap \alpha_3 = \emptyset$ and that each arc in a_i is connected to one arc from each of a_{i-1} and a_{i+1}. Denote the discrete set of points $a_{i-1} \cap a_{i+1}$ by b_i.

Starting with a decomposed curve c, push each arc of a_i into H_{α_i}, leaving the endpoints fixed. We claim that the decomposition $X - \eta(c) = \cup_{i=1}^3 X_i - \eta(c)$ is a $\star$-trisection. Since $c \cap X_i = a_{i-1} \cup a_i \subset \partial X_i$ is a collection of disjoint arcs in the boundary of X_i, the complement $\widetilde{X}_i := X_i - \eta(c)$ is diffeomorphic to X_i. By construction, the arcs a_i are simultaneously parallel

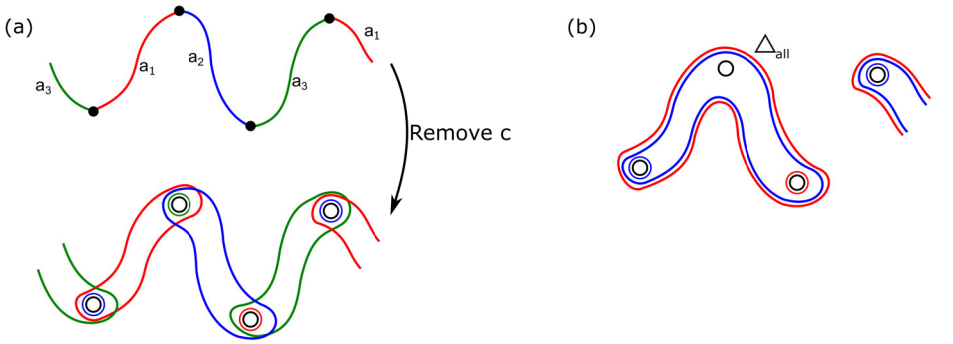

Figure 21: How a ⋆-trisection diagram changes when taking the complement of a decomposed curve in Σ.

to the boundary of H_i, thus $\widetilde{X}_i \cap \widetilde{X}_{i+1}$ is also a compression body. Hence we have a ⋆-trisection of $X - \eta(c)$.

We now describe the ⋆-trisection diagram for $X - \eta(c)$ resulting from this procedure. The trisection surface $\widetilde{\Sigma} = \cap_i \widetilde{X}_i$ is a copy of Σ with open disks removed around the endpoints of all the arcs. Start by drawing a ⋆-trisection diagram

$$(\Sigma; \alpha_1, \alpha_2, \alpha_3; \Delta_{\alpha_1 \cap \alpha_2}, \Delta_{\alpha_2 \cap \alpha_3}, \Delta_{\alpha_3 \cap \alpha_1})$$

for X together with the immersed decomposed curve $c = a_1 \cup a_2 \cup a_3$. Let $\widetilde{\Sigma}$ be the punctured surface $\Sigma - \cup_{i=1}^{3} \eta(b_i)$. Then the compression body $\widetilde{H}_i = \widetilde{X}_i \cap \widetilde{X}_{i+1}$ can be built from $\widetilde{\Sigma}$ by attaching 2-handles along the following curves (see Figure 21).

1) The original curves α_i,

2) the boundary parallel curves $\partial\eta(b_i)$ and

3) the non-boundary parallel components of $\partial\eta(a_i)$.

For each pair $(i, i+1)$, the new standard picture is given by adding extra loops in $\Delta_{\alpha_i \cap \alpha_{i+1}}$ as in Part (b) of Figure 6.2.

Remark 6.2. If X is closed and we can decompose the curve c so that $|a_i| = 1$, then the ⋆-trisection diagram given by the procedure above introduces an unnecessary curve which we can remove. The new ⋆-trisection diagram for the complement is depicted in Figure 22. To see why this is true, compress $\widetilde{\Sigma}$ along all of the original α curves. What remains is a thrice punctured surface. The two new α curves introduced by the procedure above become parallel,

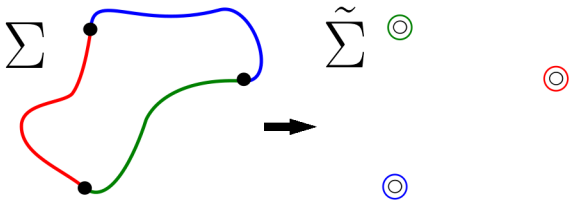

Figure 22: How the $\star$-trisection diagram changes if each $|a_i| = 1$ and $\partial X = \emptyset$.

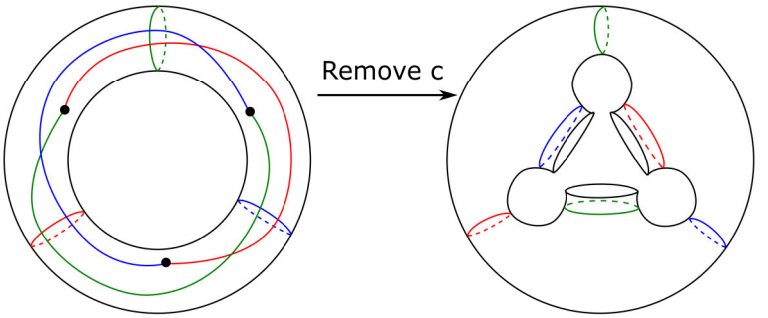

Figure 23: A trisection diagram for $S^1 \times S^3$ together with a decomposed curve c homotopic to twice the generator $S^1 \times \{pt\}$. The right picture is a $\star$-trisection diagram for the complement.

thus we can remove one of them. Figure 23 shows a concrete example of this operation.

6.1. Loops in genus one trisections

Recall that all simple closed curves in a 4-manifold X representing a fixed homotopy class $[c] \in \pi_1(X)$ are isotopic. It is therefore natural to wonder if, for simple $\star$-trisections, any two decomposed curves representing a given class $[c] \in \pi_1(X)$ are slide equivalent in the $\star$-trisection surface. We prove that this is the case for embedded curves in genus one classical trisections. The following technical proposition is key to show in Section 7 that an infinite family of genus three trisection diagrams is standard.

Proposition 6.3. Let $(\Sigma; \alpha, \beta, \gamma)$ be a genus one trisection diagram for a closed 4-manifold. Let c be an embedded decomposed curve with $|a_i| = 1$ in

Σ. Let $\{\mu, \lambda\}$ be a basis for $\pi_1(\Sigma)$ with $[\alpha] = [\mu]$. If $[c] = [m\mu + n\lambda]$, then by sliding the arcs a_i over the boundaries $b_i = a_{i+1} \cap a_{i-1}$, and sometimes sliding a_1 over α, c is slide equivalent to an immersed curve representing $[n\lambda]$ with a_1 twisting around b_3 a total of m times.

Proof. Throughout this argument β and γ will be pushed around as needed. If γ or β are in the way of sliding a_i over b_i for $i = 1, 2$, simply include them in the slide as in the left of Figure 24. Since c is embedded and $a_1 \cap \alpha = \emptyset$, the n intersections of c with α occur on $a_2 \cup a_3$. Isotope c such that $a_2 \cap \alpha = \emptyset$. Since a_1 and a_2 both miss α, we may isotope them such that a_1 is a small segment leaving b_2, a_2 is a small segment leaving b_3 with $a_1 \cup a_2$ being contained in a small disk D disjoint from $\lambda \cup \mu$. This way, all of the intersections of c with $\lambda \cup \mu$ occur on a_3. Therefore, since c is embedded in Σ, $a_3 - D$ is a properly embedded arc in $\Sigma - D$. Thus we may assume from the beginning that the trisection as well as the embedded decomposed curve are isotopic to the model in the right of Figure 24 where we have suppressed the β and γ curves. At this point in the argument, the β and γ curves cannot be assumed to lie in any kind of special position with respect to c.

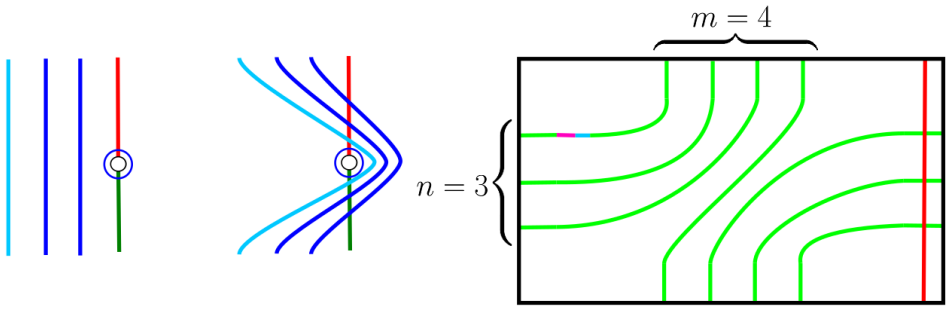

Figure 24: (left) How the β and γ curves behave as we manipulate c. (right) The initial position of embedded c with $[c] = [4\mu + 3\lambda]$.

Let w be the word in the alphabet $\{\mu, \lambda\}$ which represents $[c]$ and decompose w into three subwords w_1, w_2, w_3 such that $w = w_1 w_2 w_3$ and each w_i records the intersections of a_i with μ and λ. Initially, as described above, we have that w_1 and w_2 are empty words and w_3 is a certain permutation of the multiset $\{m\mu, n\lambda\}$ which allows a_3 to be an embedded arc. We claim that a decomposed c representing $[m\mu + n\lambda]$, $m > 0$, in such a way that w_1 and w_2 are empty words, can be slid to be a representative of $[(m-1)\mu + n\lambda]$ with w_1 and w_2 being empty words.

Suppose that c represents $[m\mu + n\lambda]$, $m > 0$ with w_1 and w_2 empty. Then since $m > 0$, let $j \geq 0$ such that $\lambda^j\mu$ is a prefix of w_3. The endpoint of a_2 connected to a_3 is b_1. We can make b_1 "move past" α and a_1 by performing the local move in Figure 25.

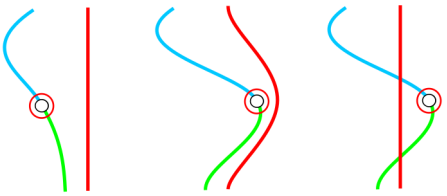

Figure 25: How b_1 moves past α or a_1 in this argument.

We can therefore move b_1 along a_3 until w_2 reads $\lambda^j\mu$, Figure 26. Using the fact that this is a genus one trisection, and the fact that $\lambda^j\mu$ is embedded, by sliding a_2 over b_2 when necessary as in Figure 27 we can commute μ past λ^j. After an isotopy of a_1 and a_2, reading from left to right in the two leftmost frames in 28, we achieve $w_1 = \mu$ and $w_2 = \lambda^j$. From this position, we can slide a_1 against α to yield $w_1 = \emptyset$ at the expense of adding a single twist of a_1 around b_3. This introduces a bigon between a_1 and λ which is easily resolved. This slide and subsequent isotopy are shown in the last 2 frames. Now it is possible to commute μ past λ^j by sliding a_2 over b_2 when

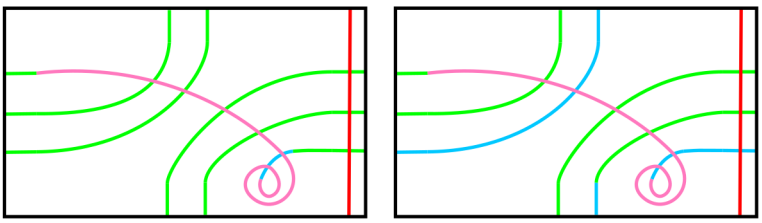

Figure 26: In this example w_2 consumes $\lambda\mu$ from w_3, accomplished by extending b_2.

necessary.

After completing this slide to eliminate μ, we can shrink a_2, removing λ^j from w_2 and appending λ^j to the front of w_3. The decomposed curve at this stage is a representative of $[(m-1)\mu + n\lambda]$ with $w_1 = w_2$ empty, so the claim is proved. By repeating this process, we can slide c to the model representative of $[n\lambda]$ below with $w_1 = w_2$ being empty and $w_3 = \lambda^l$. □

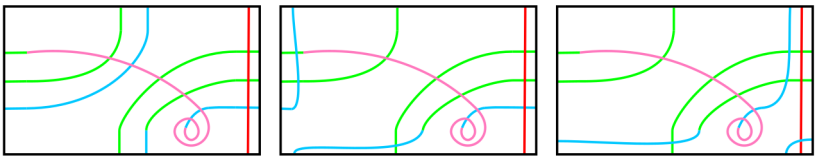

Figure 27: A depiction of an isotopy of a_2 which corresponds to the rewriting $\lambda\mu \to \mu\lambda$ in w_2.

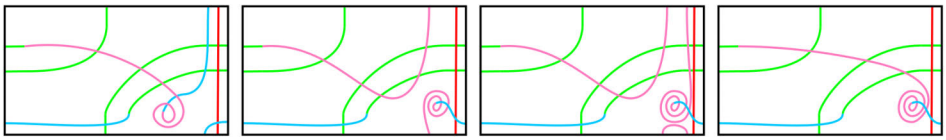

Figure 28: Eliminating μ from w by sliding a_1 over α.

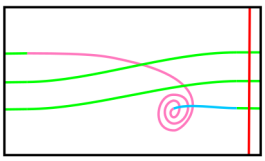

Figure 29: The final product.

Continuing the argument in Proposition 6.3. Suppose that $(\Sigma, \alpha, \beta, \gamma)$ is a genus one trisection for a simply connected 4-manifold with $[\lambda] = [\beta]$. Then we can say even more: Since $w = \lambda^n$, we may extend a_2 so that $w_2 = \lambda^n$ and $w_1 = w_3$ are empty words. Putting β back into the picture, it is now clear that we can slide λ off as well, see Figure 30. This proves the following.

Corollary 6.4. Let $(\Sigma; \alpha, \beta, \gamma)$ be a genus one trisection diagram for a simply connected closed 4-manifold. Let c be an embedded decomposed curve in Σ. Let $\{\mu, \lambda\}$ be a basis for $\pi_1(X)$ with $[\alpha] = [\mu]$ and $[\beta] = [\lambda]$. If $c = m\mu + n\lambda$, then by sliding the arcs a_i over the boundaries $b_i = a_{i+1} \cap a_{i-1}$, sometimes sliding a_1 over α, and sometimes sliding a_2 over β, c is slide equivalent to an immersed curve representing $1 \in \pi_1(\Sigma, b_2)$ with a_1 twisting around b_3 a total of m times and a_2 twisting around b_1 a total of $n - 1$ times.

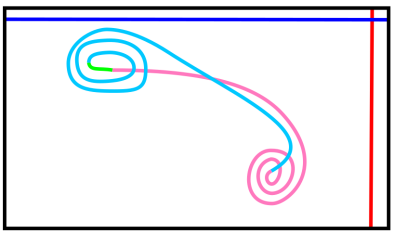

Figure 30: An immersed curve representing $1 \in \pi_1(\Sigma, b_2)$ with twists around boundary points.

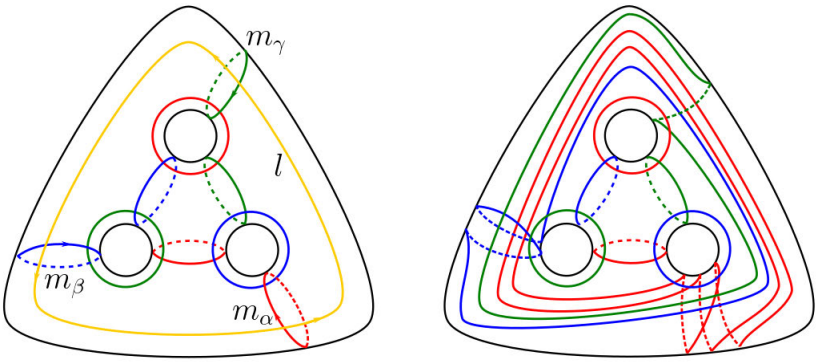

Figure 31: (left) The longitude (l) and meridian (m) for each of the three tori. (right) The diagram $D(\frac{2}{3}, \frac{1}{1}, \frac{1}{2})$.

7. Trisections of genus 3

For two irreducible fractions $\frac{a}{b}, \frac{c}{d} \in \mathbb{Q} \cup \{\frac{1}{0}\}$, define $d(\frac{a}{b}, \frac{c}{d}) := \det \left(\begin{smallmatrix} a & c \\ b & d \end{smallmatrix}\right)$. Given an ordered triple of rational numbers $\frac{a}{b}, \frac{c}{d}, \frac{p}{q} \in \mathbb{Q} \cup \{\frac{1}{0}\}$, we can consider the diagram $D(\frac{a}{b}, \frac{c}{d}, \frac{p}{q})$ as in the right side of Figure 31. Here one curve of each α, β, γ set has slope $\frac{a}{b}$, $\frac{c}{d}$, $\frac{p}{q}$, respectively, in the torus obtained by compressing the genus three surface along the two central curves of the same color as in the left side of Figure 32. The diagram $D(\frac{a}{b}, \frac{c}{d}, \frac{p}{q})$ is a trisection diagram for some closed smooth 4-manifold if and only if each pair $x, y \in \{\frac{a}{b}, \frac{c}{d}, \frac{p}{q}\}$ satisfies the inequality $|d(x, y)| \leq 1$. If the three numbers in the triplet are all distinct with $d(x, y) = \pm 1$ for all $x \neq y \in \{\frac{a}{b}, \frac{c}{d}, \frac{p}{q}\}$, then we call $\{\frac{a}{b}, \frac{c}{d}, \frac{p}{q}\}$ a **Farey triplet**. In this case, $\{\frac{a}{b}, \frac{c}{d}, \frac{p}{q}\}$ corresponds to a triangle in the Farey graph.

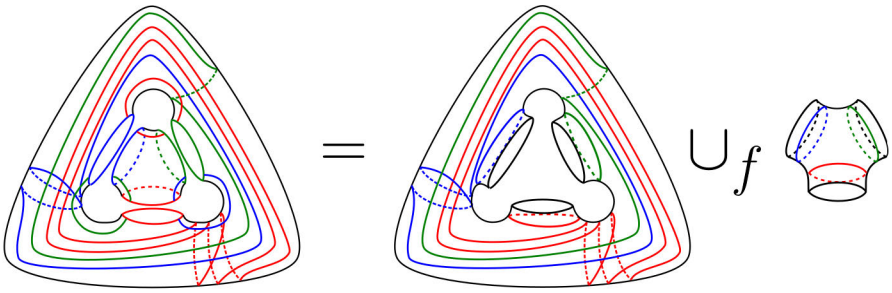

Figure 32: Decomposing X as $(S^2 \times D^2) \cup_\partial Y$ glued via some map $f : S^1 \times S^2 \to \partial Y$.

The question we will discuss now is what 4-manifolds the diagrams $D(\frac{a}{b}, \frac{c}{d}, \frac{p}{q})$ represent. Meier proved in [21] that $D(\frac{q}{p}, \frac{q}{p}, \frac{q}{p})$ is the diagram of a spun lens space $L(p, q)$. He conjectured that the only 4-manifolds admitting genus three trisections are spun lens spaces and certain connected sums of combinations of $S^1 \times S^3$, $S^2 \times S^2$, $\mathbb{CP}^2$, and $\overline{\mathbb{CP}^2}$. We will call the latter combinations standard manifolds. Note that $D(\frac{a}{b}, \frac{c}{d}, \frac{p}{q})$ is simply connected whenever $\{\frac{a}{b}, \frac{c}{d}, \frac{p}{q}\}$ contains two or three distinct numbers. Thus, such diagrams must represent standard manifolds if we expect the conjecture to be true. We prove that this is indeed the situation.

Theorem 7.1. Let $\frac{a}{b}, \frac{c}{d}, \frac{p}{q} \in \mathbb{Q} \cup \{\frac{1}{0}\}$ satisfying $|d(x, y)| \leq 1$ for all $x, y \in \{\frac{a}{b}, \frac{c}{d}, \frac{p}{q}\}$. Then $D(\frac{a}{b}, \frac{c}{d}, \frac{q}{p})$ describes a trisection diagram for

1) either $\mathbb{CP}^2 \# \mathbb{CP}^2 \# \overline{\mathbb{CP}^2}$ or $\mathbb{CP}^2 \# \overline{\mathbb{CP}^2} \# \overline{\mathbb{CP}^2}$ if $\{\frac{a}{b}, \frac{c}{d}, \frac{p}{q}\}$ is a Farey triplet,
2) either $S^2 \times S^2$ or $S^2 \widetilde{\times} S^2$ if $\{\frac{a}{b}, \frac{c}{d}, \frac{p}{q}\} = \{x, y\}$ with $d(x, y) = \pm 1$,
3) a spun lens space if $\{\frac{a}{b}, \frac{c}{d}, \frac{p}{q}\} = \{x\}$.

To find out the specific 4-manifold the above diagrams represent, it is enough to compute its intersection matrix using [11] or [13].

Proof. The third part was done by Meier in [21]. Denote by X the 4-manifold represented by the diagram $D(\frac{a}{b}, \frac{c}{d}, \frac{p}{q})$. Notice that we can decompose the genus three surface in Figure 31 into a thrice punctured sphere and a thrice puntured torus glued together along their boundaries, see Figure 32. Theorem 5.3 implies that X decomposes as the union $X = (S^2 \times D^2) \cup_\partial Y$ for some 4-manifold Y.

Remark 6.2 implies that the $\star$-trisection diagram corresponding to Y can be viewed as the result of taking the complement of a decomposed curve in

a genus one trisection. So if $\{\frac{a}{b}, \frac{c}{d}, \frac{p}{q}\}$ is a Farey triplet, the diagram for Y implies that Y is the complement of a curve c in $\mathbb{CP}^2$ (or $\overline{\mathbb{CP}^2}$). Since $\mathbb{CP}^2$ is simply connected, we can isotope c to lie inside a small 4-ball and so $Y = \mathbb{CP}^2 \# (S^2 \times D^2)$. Hence X is the connected sum of $\mathbb{CP}^2$ with a sphere bundle over the sphere. Suppose now $\{\frac{a}{b}, \frac{c}{d}, \frac{p}{q}\} = \{x, y\}$ with $d(x, y) = \pm 1$, then Remark 6.2 implies that Y is the complement of a decomposed loop in a genus one trisection for S^4. Thus $Y = S^4 - (S^1 \times B^3)$ and X is a copy of $S^2 \times S^2$ or $S^2 \widetilde{\times} S^2$.

We have shown the 4-manifolds associated to the trisection diagrams $D(\frac{a}{b}, \frac{c}{d}, \frac{p}{q})$ are diffeomorphic to standard ones. To figure out which ones specifically, it is sufficient to compute the intersection form Q_X. The intersection form of X, computed from $D(\frac{a}{b}, \frac{c}{d}, \frac{p}{q})$ using [11], is given by

$$Q_X = \begin{bmatrix} \frac{bd}{ad-bc} & -1 & \frac{b(cq-dp)}{bc-ad} \\ -1 & 0 & 0 \\ \frac{b(cq-dp)}{bc-ad} & 0 & \frac{(bp-aq)(cq-dp)}{bc-ad} \end{bmatrix}.$$

In the case that $\frac{c}{d} = \frac{p}{q}$, notice the third column and third row become zero and we are left with the intersection form $Q_X = \begin{bmatrix} \frac{bd}{ad-bc} & -1 \\ -1 & 0 \end{bmatrix}$ which is equivalent to the intersection form for $S^2 \times S^2$ when bd is even and to $S^2 \widetilde{\times} S^2$ when bd is odd. If all rationals are distinct, then without loss of generality suppose that $d(\frac{a}{b}, \frac{c}{d}) = 1$. Because $\{\frac{a}{b}, \frac{c}{d}, \frac{p}{q}\}$ is a Farey triple, we know that $\frac{p}{q} = \frac{a \pm c}{b \pm d}$. This gives

$$Q_X = \begin{bmatrix} bd & -1 & b \\ -1 & 0 & 0 \\ b & 0 & \mp 1 \end{bmatrix}.$$

By inspection, one determines that Q_X is equivalent to $\langle 1 \rangle \oplus \langle \mp 1 \rangle \oplus \langle -1 \rangle$. □

7.1. Farey trisections are standard

We will now demonstrate that in cases 1 or 2 of Theorem 7.1, the diagrams $D(\frac{a}{b}, \frac{c}{d}, \frac{p}{q})$ are actually reducible and thus standard.

Theorem 7.2. Let $\{\frac{a}{b}, \frac{c}{d}, \frac{p}{q}\} \subset \mathbb{Q} \cup \{\frac{1}{0}\}$ with $d(x, y) \leq 1$ for each $x, y \in \{\frac{a}{b}, \frac{c}{d}, \frac{p}{q}\}$. If at least two of these fractions are distinct, then $D(\frac{a}{b}, \frac{c}{d}, \frac{p}{q})$ is handle slide equivalent to the standard diagram for $T \# S$ where $T \in \{S^4, \mathbb{CP}^2, \overline{\mathbb{CP}^2}\}$ and $S \in \{S^2 \times S^2, S^2 \widetilde{\times} S^2\}$.

Proof. Decompose $D(\frac{a}{b}, \frac{c}{d}, \frac{p}{q})$ into two pieces as suggested by Figure 32; let D' denote the thrice punctured torus component of this decomposition and let P denote the thrice punctured sphere component. Notice that this $\star$-trisection D' is a diagram for the complement of an embedded curve in a simply connected 4-manifold. Specifically, D' is the result of taking the complement of the $c = \lambda$ curve in a genus 1 trisection with curves $\alpha = a\lambda + b\mu$, $\beta = c\lambda + d\mu$, and $\gamma = p\lambda + q\mu$ where the curve c has been decomposed as suggested by the left side of Figure 32. By Corollary 6.4, the decomposed curve c is slide equivalent to an immersed decomposed curve c' representing the trivial curve where some of the arcs twist around the boundary points, as in the last frame of Figure 30. In particular, α and β are disjoint from c'. Using the fact that c' represents the trivial loop, we can slide γ against b_3 until γ is disjoint from c' also. Thus there is a curve δ separating c' from α, β, γ. By surgering D' along δ we get two components. Let Q be the component coming from the side of δ containing c' and let T be the torus component containing α, β, γ. Notice that $S = Q \cup_f P$, with the attaching map f given by the a_i, is a genus two trisection of a closed 4-manifold with an intersection form of full rank. By the work of Meier and Zupan [23], S is a trisection diagram for $S^2 \times S^2$ or $S^2 \widetilde{\times} S^2$. The component T is a genus one trisection of a simply connected closed 4-manifold: $S^4, \mathbb{CP}^2$ or $\overline{\mathbb{CP}^2}$. □

Remark 7.3 (Spun lens spaces). In [21], Meier asked if the diagrams $D(\frac{p}{q}, \frac{p}{q}, \frac{p}{q})$ and $D(\frac{1}{q}, \frac{1}{q}, \frac{1}{q})$ depict diffeomorphic trisections. With this in mind, we can proceed as in Theorem 7.2 and see that Proposition 6.3 implies that the diagrams $D(\frac{p}{q}, \frac{p}{q}, \frac{p}{q})$ and $D(\frac{1}{q}, \frac{1}{q}, \frac{1}{q})$ are handle slide equivalent to diagrams which are identical outside of the regular neighborhood of a γ curve, say γ_0. In this annulus $\nu(\gamma_0)$, the diagrams differ by their α curves, where one twists q times around this annulus and the other twists once (see Figure 33). This motivates the following question about uniqueness of trisection diagrams for 1-surgeries.

Question 7.1. Let c be an embedded loop in a 4-manifold X represented by a (possibly immersed) decomposed curve in the genus g trisection surface. If $|a_i| = 1$ in the decomposition of the curve, is the resulting genus $g + 2$ trisection diagram for $(X - \eta(c)) \cup (S^2 \times D^2)$, with a specific choice of framing in $\mathbb{Z}/2\mathbb{Z}$, unique up to handle slides and diffeomorphisms of the surface? In particular, are the trisections given by the diagrams in Figure 33 diffeomorphic?

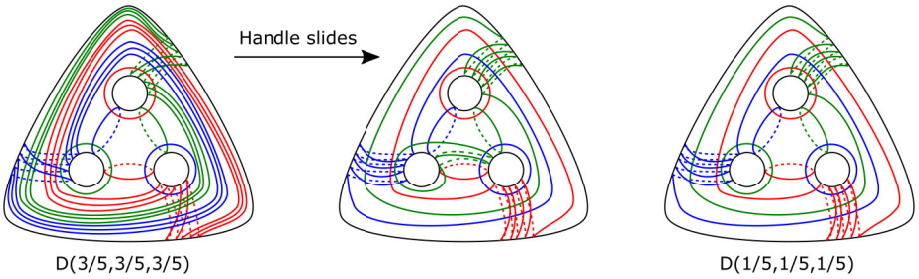

Figure 33: How the handle slides described in Proposition 6.3 change the diagram $D(\frac{3}{5}, \frac{3}{5}, \frac{3}{5})$. The middle and right diagrams difeer by removing an embedded $S^2 \times D^2$ and regluing it using a power of the Gluck twist map. Question 7.1 asks if whether these two diagrams depict diffeomorphic trisections for even powers the Gluck twist map.

8. Surface surgery

The main goal of this section is to use $\star$-trisections to draw diagrams for closed 4-manifolds obtained by various kinds of surgery. Drawings for these 4-manifolds could be theoretically derived using previous work on relative trisections. However, the genus of these diagrams will often be large. For example, in [9], a genus seven trisection of $T^2 \times S^2$ was obtained by taking the double of a genus 3 relative trisection for $T^2 \times D^2$. In Figure 18, we used a genus one $\star$-trisection for $T^2 \times D^2$ to draw a genus four trisection for $T^2 \times S^2$. This section provides diagrams for the Cacime Surface (Section 8.2), and algorithms to perform Fintushel-Stern knot surgery (Section 8.3) and torus surgeries (Section 8.4) such as Logarithmic transforms and Luttinger transforms. The careful reader might observe that the diagrams for these transformations change by concatenating a fixed picture or by changing some loops in a high enough stabilization of the original trisection diagram. Thus to study the behavior of 4-manifold invariants under surface surgery, it could be worthwhile to explore each local modifications in detail.

8.1. Embedded surfaces and their complements

Let $X = X_1 \cup X_2 \cup X_3$ be a $\star$-trisected 4-manifold and let $F \subset X$ be an embedded closed surface. Following Meier and Zupan [24], we say that F is in $(g; c_1, c_2, c_3)$**-bridge position** with respect to the $\star$-trisection if, for each $i \neq j$, $\mathcal{D}_i = F \cap X_i$ is a collection of c_i trivial disks in X_i, and the arcs

$\mathcal{D}_i \cap \mathcal{D}_j$ form a trivial b-tangle in the compression body $C_{ij} = X_i \cap X_j$. As a consequence, the intersection $F \cap (X_1 \cap X_2 \cap X_3)$ is a collection of $2b$ points.

Given a $\star$-trisection diagram $(\Sigma; \alpha, \beta, \gamma)$, we can decode[7] a $(b; c_1, c_2, c_3)$-bridge trisection of F by three sets of b embeded arcs s_α, s_β, s_γ in Σ corresponding to the shadows of the trivial tangles $F \cap C_\varepsilon$, $\varepsilon \in \{\alpha, \beta, \gamma\}$. The shadow arcs have $2b$ common endpoints $t = F \cap \Sigma$. We consider the arcs in s_ε to be disjoint from the loops in ε. Thus, isotopy of the arcs $F \cap C_\varepsilon$ relative to their boundaries corresponds to sliding the shadows s_ε over ε. For each pair $(\varepsilon, \mu) \in \{(\alpha, \beta), (\beta, \gamma), (\gamma, \alpha)\}$, the arcs s_ε, s_μ in Σ determine a c_i-component unlink in bridge position with respect to the Heegaard splitting $C_\varepsilon \cup_\Sigma C_\mu$, where $i \in \{1, 2, 3\}$ is the index corresponding to the pair (ε, μ). For more details and examples of bridge trisections see [20, 22, 24].

Given a bridge trisected surface $F \subset X$, there is an obvious $\star$-trisection for the complement $X - \eta(F)$ given by $\widetilde{X}_i = X_i - \eta(\mathcal{D}_i)$, $i = 1, 2, 3$. Let s_α, s_β, s_γ be a set of shadows for F in the $\star$-trisection diagram $(\Sigma; \alpha, \beta, \gamma)$. A $\star$-trisection diagram for $X - \eta(F)$ is given by $(\widetilde{\Sigma}; \widetilde{\alpha}, \widetilde{\beta}, \widetilde{\gamma})$ where $\widetilde{\Sigma} = \Sigma - \eta(t)$ is a copy of Σ with $|t|$ disks removed, and for each $\varepsilon \in \{\alpha, \beta, \gamma\}$, $\widetilde{\varepsilon} = \varepsilon \cup \varepsilon'$ where the extra loops in ε' are obtained from the non-boundary parallel components of $\partial\eta\,(s_\varepsilon \cup \eta(t))$. Using the notation of Remark 3.9, the curves in ε' correspond to new curves of type 2.

See Figure 34 for a concrete example. In the rest of the section we will see how we can use $\star$-trisection diagrams to draw diagrams for surgeries along bridge trisected surfaces.

Remark 8.1. It is important to mention that this decomposition was previously discussed by Kim and Miller in [17]. The authors of [17] observed that the above $\star$-trisection is a classic trisection only when F is a 2-sphere. To obtain a classical relative trisection, Kim and Miller performed a sequence of "boundary-stabilizations" to the $\star$-trisection above. This procedure increases the complexity of the trisection surface in a controlled way, and in principle can also be used to perform surgery along surfaces following the methods in this section.

Example 8.2 (Trisecting the 4-torus). Figure 34 shows a $\star$-trisection diagram for $T^3 \times [0, 1]$ obtained from removing an open neighborhood of $T^2 \times \{0\}$ inside $T^2 \times D^2$. We can poke this diagram in order to satisfy the boundary conditions of Lemma 5.1. To build T^4, we glue two copies of $T^3 \times [0, 1]$ along the identity in their boundaries. Diagram-wise, this corresponds

[7] This is a consequence of Lemma 3.5.

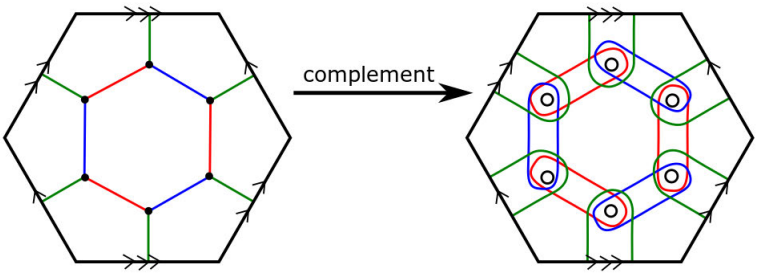

Figure 34: (left) A bridge trisection for $T^2 \times \{pt\}$ inside $T^2 \times D^2$. (right) A $\star$-trisection for $T^2 \times S^1 \times [0,1] = T^3 \times [0,1]$.

to 'double' the poked diagram for $T^3 \times [0,1]$ and add some extra loops using Remark 5.2. For each color $\varepsilon \in \{\alpha, \beta, \gamma\}$, we draw embedded arcs disjoint from ε cutting the compressed surface Σ_ε into a disjoint union of disks. The new curves are given by gluing two copies of the arcs, one on each surface, along their endpoints as in Figure 36. The resulting diagram represents a (10;4)-trisection for the 4-torus.

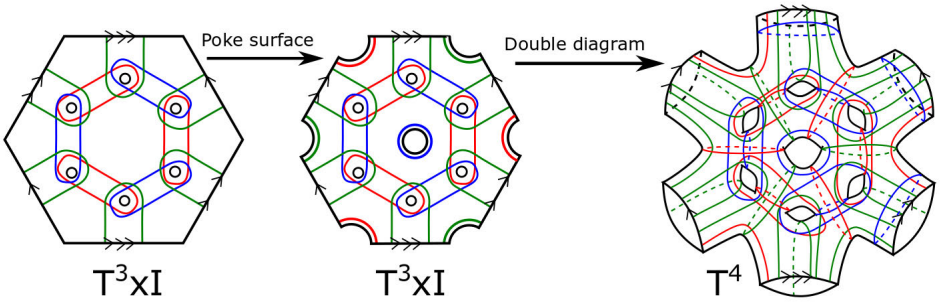

Figure 35: Trisecting the 4-torus.

The following proposition explains how obtain a trisection for fiber sums of two 4-manifolds.

Proposition 8.3. Let X and X' be two closed connected 4-manifolds. Let $\tau = W_1 \cup W_2 \cup W_3$ (resp. τ') be a $(g; k_1, k_2, k_3)$-trisection for X (resp. X'). Suppose $F \subset X$ (resp. $F' \subset X'$) is a closed embedded surface in $(b; c_1, c_2, c_3)$-bridge position with respect to τ (resp. τ'). Suppose $F \cdot F = F' \cdot F'$ and that the cell decompositions in F and F' induced by the bridge trisections agree; in other words, $b = b'$ and $c_i = c_i'$ for $i = 1, 2, 3$. Then the fiber sum of X and

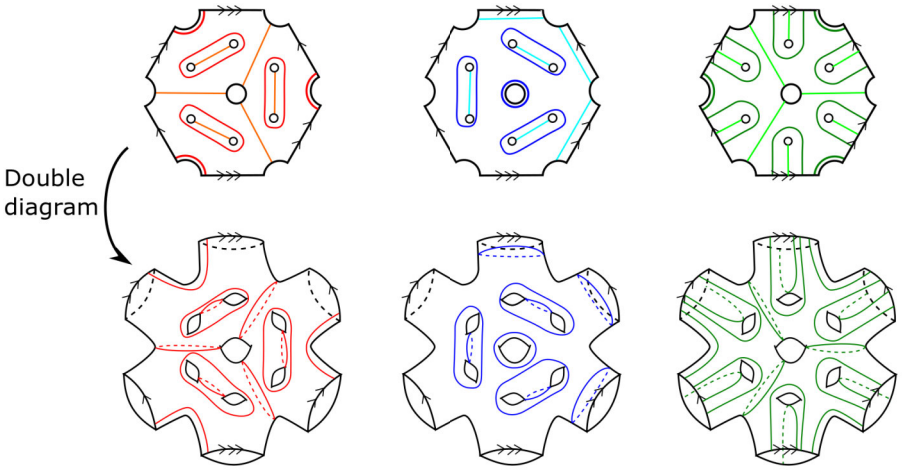

Figure 36: How to double the diagram for $T^3 \times [0,1]$.

X' along F and F', denoted by $X \natural X'$, admits a $(G; K_1, K_2, K_3)$-trisection where $G = g + g' + 2b - 1$ and $K_i = k_i + k'_i + c_i$.

Proof. The condition $F \cdot F = F' \cdot F'$ is so that the gluing map $f : \partial\eta F \to \partial\eta F'$ exists. To trisect the fiber sum of X and X' one must trisect the complements $X - \eta(F)$ and $X' - \eta(F')$ using the bridge trisections. Since $b = b'$ and $c_i = c'_i$ for $i = 1, 2, 3$, the handle decompositions in $\partial\eta(F)$ and $\partial\eta(F')$ induced by the $\star$-trisections agree. Thus we can apply Lemma 5.1 and obtain a trisection for $X \natural X'$. The $\star$-trisection surface for $X - \eta(F)$ is connected of genus g and $2b$ boundary components; similarly for $X' - \eta(F')$. By Remark 5.2, the trisection surface for $X \natural X'$ is a closed surface of genus $G = g + g' + 2b - 1$.

To determine the value of each K_i we need to dive into the proof of Lemma 5.1. Fix $i \in \{1, 2, 3\}$, the 4-manifold piece $W_i - \eta(F)$ is determined by the tuple $(\Sigma; \Delta^1, \Delta^0, \Delta_{all})$ as in Remark 3.9; similarly for $W'_i - \eta(F')$. By definition of bridge trisection, $F \cap \partial W_i$ is a c_i component unlink in bridge position. By construction, Δ_{all} contains separating curves breaking Σ as the connected sum of a genus g closed surface and a c_i spheres, each of them with positive even number of boundary components. Each sphere corresponds to a component of the unlink $F \cap \partial W_i$. The curves (Δ^0, Δ^1) in the genus g surface determine a 1-handlebody with k_i 1-handles. For each planar surface, the curves (Δ^0, Δ^1) are only of type 2 which determine 4-dimensional pieces that get glued with other 4-dimensional pieces coming from $W'_i - \eta(F')$. After

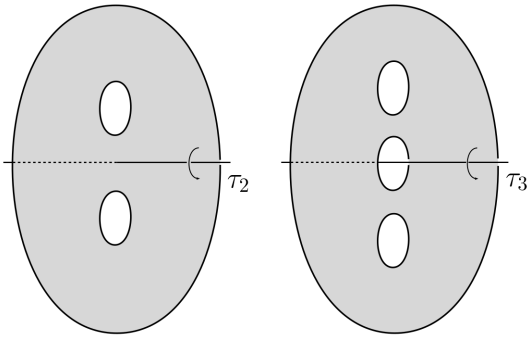

Figure 37: The involutions τ_2 and τ_3.

gluing each planar surface determines a copy of $S^1 \times B^3$ (see paragraph 4 of the proof of Lemma 5.1). Thus, as explained in paragraph 3 of the proof of Lemma 5.1, the glued 4-manifold piece $W_i \cup W_i'$ is diffeomorphic to $\natural_{K_i} S^1 \times B^3$ where $K_i = k_i + k_i' + c_i$. □

8.2. Cacime surface

Let F_2, F_3 be oriented surfaces of genus two and three, respectively. Define $\tau_i : F_i \to F_i$ to be involutions as in Figure 37. Define the Cacime Surface to be the quotient $C = F_2 \times F_3/\tau_2 \times \tau_3$. Following Chapter 4.2 of [2], C is diffeomorphic to a fiber sum of F_2 bundles over T^2

$$C = \left(F_2 \times T^2\right) \natural \left(F_2 \times S^1 \times [0,1]\right) / \widetilde{\tau}_2,$$

here $\widetilde{\tau}_2(x,t) = (\tau_2(x), t)$ is a diffeomorphism of $F_2 \times S^1$. To obtain a trisection diagram for C we follow the following three steps drawn in Figures 38, 39, 40, 41, 42 and 43

1) Draw a genus 5 Heegaard splitting for $F_2 \times S^1$ and perform Koenig's algorithm [19] to draw a $(21; 6, 6, 11)$-trisection diagram for $X_f = (F_2 \times S^1) \times [0,1]/f$ for $f \in \{id, \widetilde{\tau}_2\}$.

2) Notice that $F_2 \times \{pt\}$ can be seen in the Heegaard splitting for $F_2 \times S^1$ and use this to draw a system of shadows of a $(5; 1, 1, 1)$-bridge trisection for $F_2 \times \{pt\} \times \{pt\}$.

3) Apply the method in Section 8.1 to $\star$-trisect the complements $X_f - \eta(F_2)$ and tube the corresponding boundaries using the Pasting

Lemma to obtain a $(51; 13, 13, 23)$-trisection diagram for C (See Proposition 8.3).

Koenig showed in [19] that his algorithm always results in a trisection which can be destabilized. Here, we can destabilize ten times (five on each X_f) and get a $(41; 13)$-trisection for the Cacime Surface. This trisection will yield a handle decomposition with one 0-handle, 13 1-handles, 28 2-handles, 13 3-handles and one 4-handles. This picture resembles the handle diagram in Figure 4.17 of [2]. Thus we think of the Pasting Lemma as the trisection analog of the Roping Method for handle decompositions.

Question 8.1. Is there an interpretation for the phrase "upside-down trisection"? If so, is there a different method of gluing two $\star$-trisected 4-manifolds besides the one in Lemma 5.1?

8.3. Knot surgery

Let K be a knot in S^3, and let m denote a meridian of K. Let M_K be the 3-manifold obtained by 0-surgery along K. Notice that m can be viewed as a circle in M_K and that the torus $T_m = m \times S^1 \subset M_K \times S^1$ has self-intersection zero. Let X be a 4-manifold containing an embedded torus T with self-intersection zero. Denote by X_K the fiber sum

$$X_K = X \natural_{T=T_m} (M_K \times S^1).$$

Here, we glue the complement of the corresponding thickened tori along a diffeomorphism preserving $\{pt\} \times \partial D^2$. Fintushel and Stern introduced the knot surgery operation in [12] to build exotic copies of smooth 4-manifolds by controlling the change of the Seiberg-Witten invariants using the Alexander polynomial of K.

The goal of this subsection is to describe how to draw trisection diagrams for X_K. Figures 44, 45, 46, 47 and 48 show the steps taking K to be the trefoil knot.

Let K be a knot in S^3. Find a Heegaard splitting for S^3 such that K can be isotoped to be inside one of the handlebodies intersecting one meridian disk exactly in one point. In order to do this one can consider a tunnel system for K as in Figure 44. Project K onto the Heegaard surface F in such a way that is an embedded circle in F and the framing induced by the surface is the 0-framing on K. By construction, we can find a Heegaard diagram $(F; a, b)$ such that an isotopic copy of m belongs to a and K is disjoint from

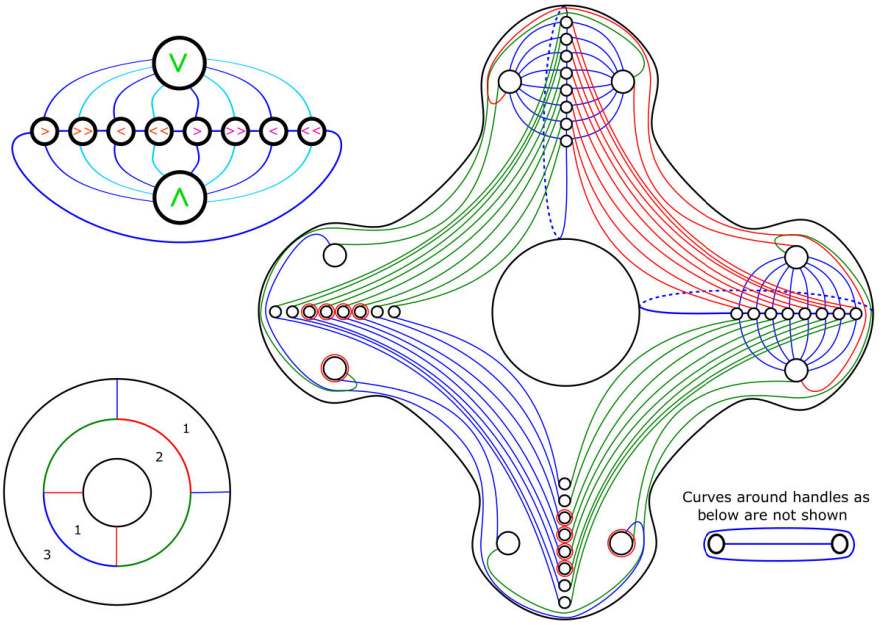

Figure 38: Genus five Heegaard splitting for $F_2 \times S^1$ and a genus 21 trisection diagram for $X_{id} = F_2 \times T^2$. Both diagrams are drawn in punctured surfaces with the correct identifications on the boundaries. The bottom left annulus is a diagrammatic representation of the trisection for X_{id}. The colored arcs in the core of the annulus correspond to thickened punctured Heegaard surfaces, and the rest of the arcs are copies of the 3-dimensional handlebodies of the original Heegaard splitting. For more detailes see [19].

all other elements of a. The pink circle in Figure 44 are possible choices for the meridian m as subsets of F. A Heegaard diagram for M_K is given by $(F; a', b)$ where $a' = (a - m) \cup K$. Furthermore, the loop m as a subset of F corresponds to the meridian of K inside M_K as in Figure 44.

Now perform Koenig's algorithm [19] to draw a trisection diagram $(\Sigma; \alpha, \beta, \gamma)$ for $M_K \times S^1$ using $(F; a', b)$. Our choice of m as a subset of F allows us to see a bridge position for $T_m = m \times S^1$. To see this recall that Σ is obtained by four copies of F tubed as in Figure 45. Draw m on each copy of Σ and pick four distinct points on each circle. Then push-off T_m away from $F \times S^1$ fixing the 16 selected points. This procedure gives us the bridge trisection of T_m with 8 bridges as in Figure 45.

Now let T be a torus with self-intersection zero embedded in a 4-manifold X. Suppose T is in bridge position with respect to some trisection of X.

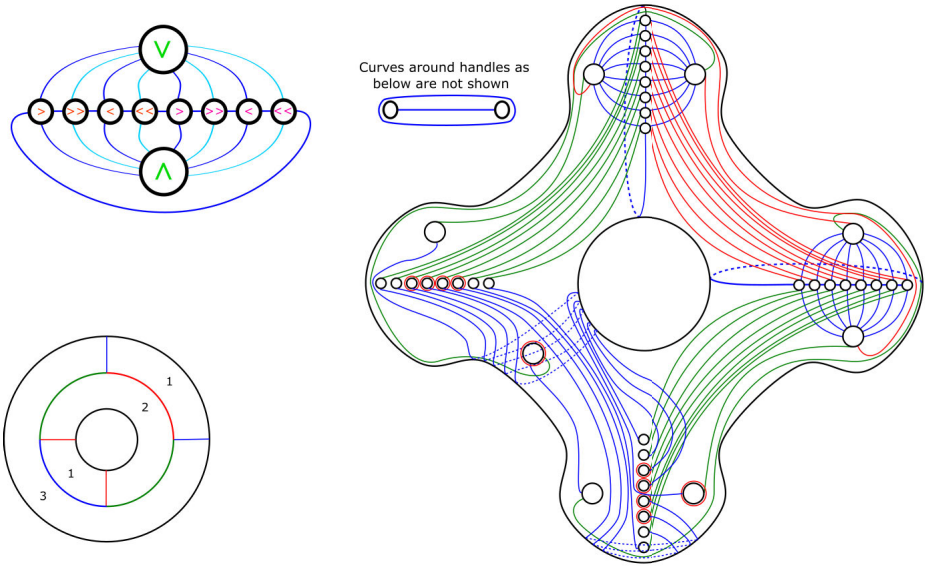

Figure 39: A genus 21 trisection diagram for X_{τ_2}. Notice the twist on some of the blue arcs is decoding the action of τ_2 in the Heegaard splitting of $F_2 \times S^1$.

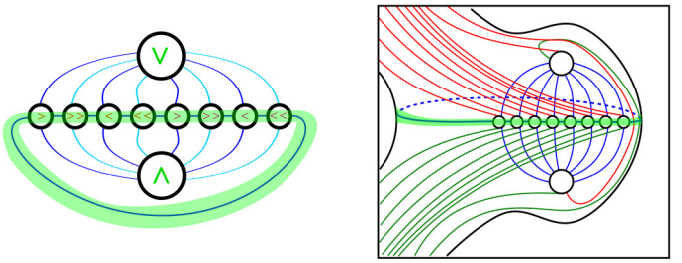

Figure 40: The green shaded area corresponds to a copy of $F_2 \times \{pt\}$ inside the Heegaard splitting for $F_2 \times S^1$ (left) and $F_2 \times \{pt\} \times \{pt\}$ in X_f.

There are two approaches we can take in order to draw a trisection diagram for X_K.

The first approach to trisect X_K is to perturb[8] both bridge trisections for T_m and T until the new bridge trisections induce the same cell decomposition on both T_m and T. Then, to draw a trisection for X_K we

[8]See [24].

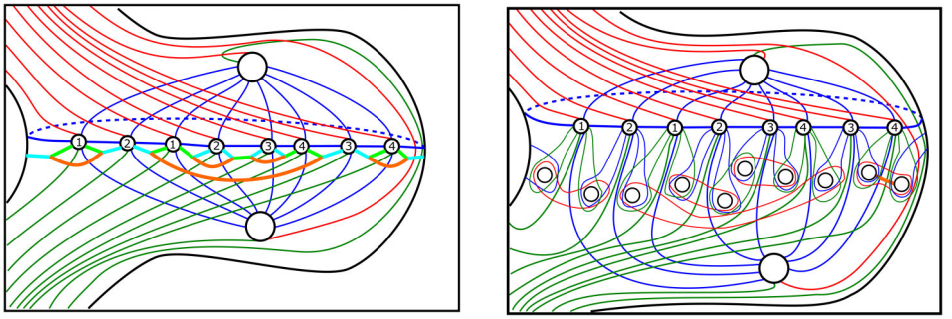

Figure 41: Local models for the bridge trisection of $F_2 \times \{pt\} \times \{pt\}$ in X_f (left), and the $\star$-trisection diagram for its complement (right).

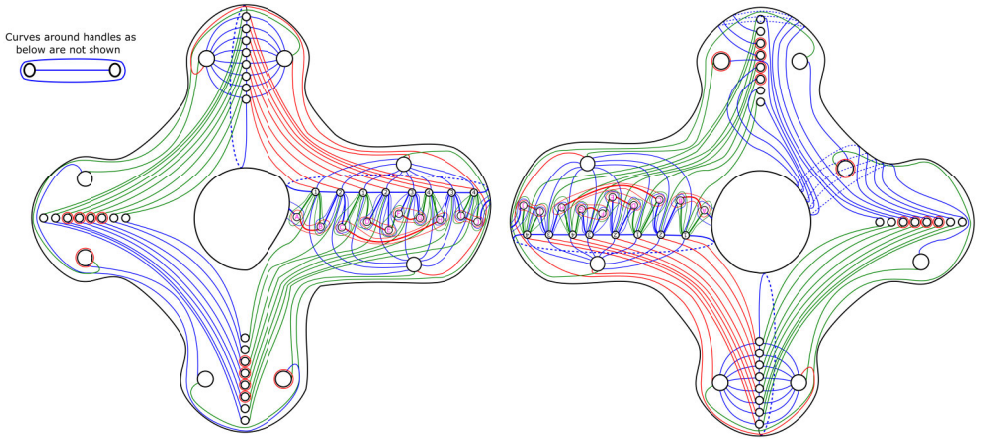

Figure 42: Genus 51 trisection diagram of the Cacime surface.

have to draw the $\star$-trisection diagrams for the corresponding surface complements following Section 8.1 and tube them using the Pasting Lemma as we did for the Cacime Surface.

The second approach to trisect X_K is to glue a copy of $T^3 \times [0,1]$ in such a way that the new boundary has a nice S^1-fibration with fiber a copy of the surface $T_m \times \{pt\}$ (similarly for T). In order to do this, draw the cell decomposition induced by the bridge trisection on the torus T_m (see Figure 46). This picture can be thought as a bridge trisection for $T_m \times \{0\}$ inside $T_m \times D^2$. Thus we can draw a $\star$-trisection diagram for $T_m \times S^1 \times [0,1]$ with one boundary having the same handle decomposition as the $\star$-trisection in Figure 45 and other boundary a S^1-fibration with fiber $T_m \times \{pt\}$. This

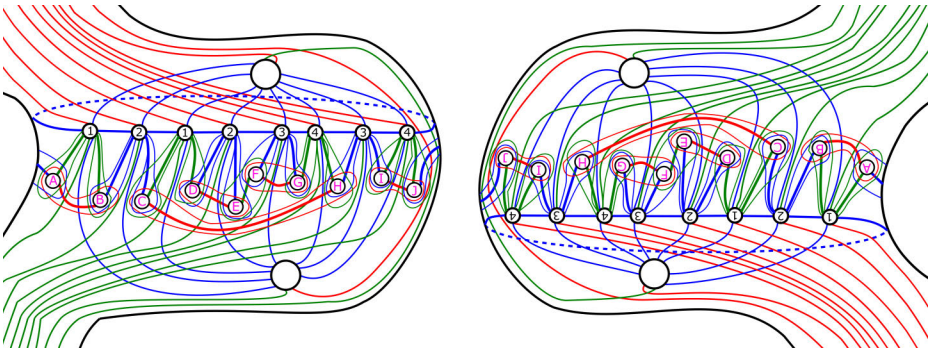

Figure 43: A close-up of the above trisection. The disks with common labels are identified as shown. Notice that some curves can be erased as in Figure 48.

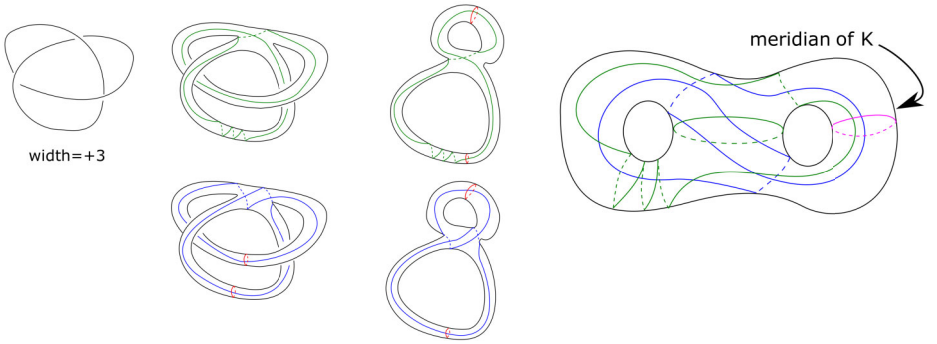

Figure 44: Heegaard diagram for M_K with K a trefoil knot.

new trisection is drawn in Figure 46. Now tube this new ⋆-trisection with the trisection for the complement of T_m in $M_K \times S^1$ to obtain a classical relative trisection (with empty binding) with a copy of T_m as the fiber on its boundary, as desired. Notice the appearance of sphere components in the compressed surfaces Σ_α, Σ_β and Σ_γ, thus some curves are redundant (see Figure 47). The final trisection diagram is depicted in Figure 48. After performing a similar process to the bridge trisection of T in X one, in theory, can perform Pasting Lemma one last time to draw a trisection for X_K.

The advantage of the second method is that any diffeomorphism of the form $f \times id_{S^1} : T_m \times \partial D^2 \to T \times \partial D^2$ can be used to perform the fiber sum.

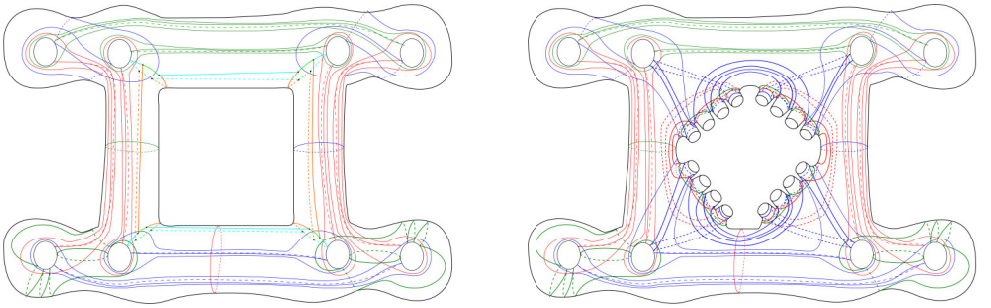

Figure 45: Bridge trisection diagram for $T_m \subset M_K \times S^1$. After an isotopy, we draw a $\star$-trisection diagram for the complement $(M_K \times S^1) - (T_m \times D^2)$.

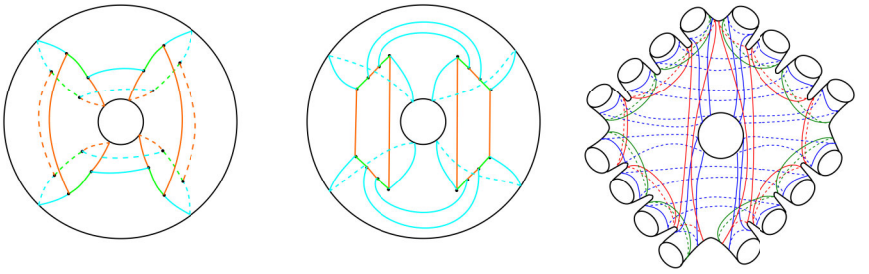

Figure 46: (left and middle) The cell decomposition induced by the bridge trisection on T_m, notice that also describes a bridge trisection for $T_m \times \{0\} \subset T_m \times D^2$. (right) The associated $\star$-trisection for the complement of this bridge trisected surface.

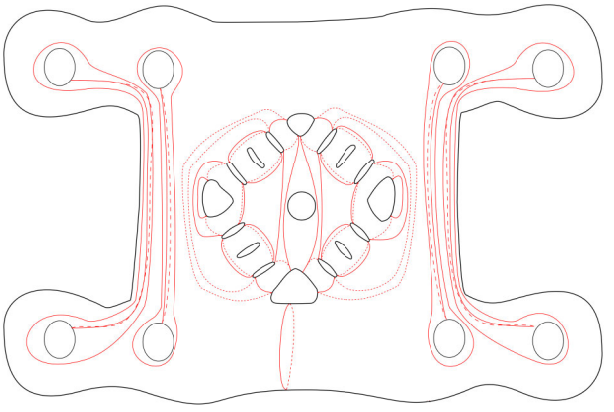

Figure 47: Red loops after performing the pasting lemma. Notice that they are some redundancies.

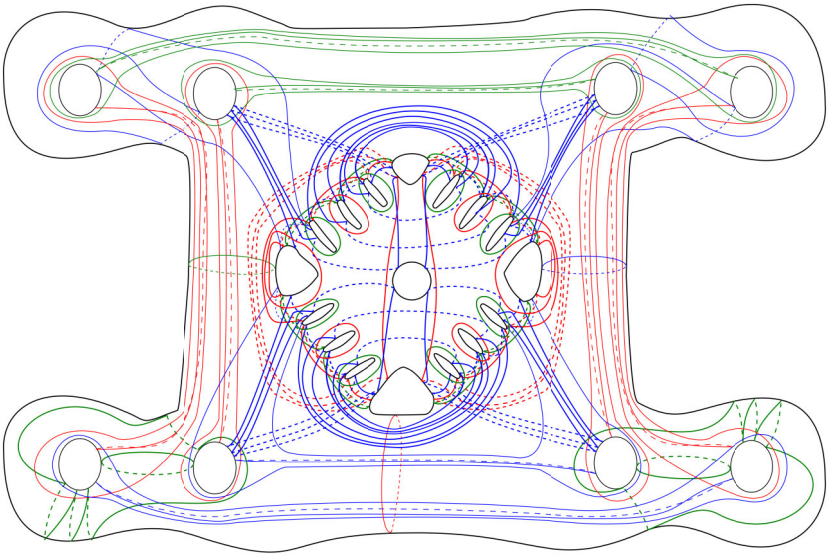

Figure 48: A trisection diagram for the complement of $T_m \times S^1$ inside $M_K \times S^1$ with boundary admitting a S^1-foliation with fiber $T_m \times \{pt\}$. To perform knot surgery, we must attach this diagram to the complement of a torus in X.

8.4. Torus surgery

Let F be an embedded torus with trivial tubular neighborhood in a $\star$-trisected 4-manifold X. The goal of this subsection is to describe how to draw trisection diagrams for all the 4-manifolds $X_{F,g} := (X - \eta(F)) \cup_g (T^2 \times D^2)$ where $g : \partial\eta(F) \to T^3$ is an isotopy class of homeomorphism of T^3. In principle, there are $SL_3(\mathbb{Z})$ many such maps.

Suppose F is in $(b; c_1, c_2, c_3)$-bridge position with respect to the given trisection of X. Begin by performing the construction of a $\star$-trisection for the complement of F in X as in Section 8.1. The handle decomposition on the boundary of the new $\star$-trisection for $X - \eta(F)$ is rather complicated. To overcome this problem, we can paste our diagram for $X - \eta(F)$ with a special diagram for $T^3 \times [0, 1]$. The bridge trisection on F induces a cell decomposition on the 2-dimensional torus. Given any such cell decomposition, we can draw a bridge position for $T^2 \times \{0\}$ in $T^2 \times D^2$ inducing the same cell decomposition. We can then draw a $\star$-trisection diagram for $T^3 \times [0, 1]$ with one boundary having the same handle decomposition as the trisection for $X - \eta(F)$. We will refer to such $\star$-trisections by τ_0. Figures 34 and 46

show examples of the τ_0 $\star$-trisections for specific cell decompositions of the 2-torus.

Gluing τ_0 to the $\star$-trisection of $X - \eta(F)$ maintains the diffeomorphism type of the complement fixed, and replaces the restrictive handle decomposition in the boundary with the S^1-foliation $F \times S^1$ with fiber an isotopic copy of $F \times \{pt\}$. We can now apply Pasting Lemma to this new trisection of $X - \eta(F)$ using diffeomorphisms of the form $g = f \times id_{S^1}$ for some homeomorphism $f : F \to F$. We think of this kind of gluing g as acting on the standard basis for $H_1(T^3, \mathbb{Z})$ via the matrix $\left(\begin{smallmatrix} a & b & 0 \\ c & d & 0 \\ 0 & 0 & 1 \end{smallmatrix}\right)$.

Denote by τ_{23} the relative trisection diagram of Example A.3. This diagram yields a relative trisection for $T^3 \times [0,1]$ with closed trisection surface such that the S^1-foliation induced in $\partial(T^3 \times [0,1])$ has page $S^1 \times S^1 \times \{pt\}$ in $T^3 \times \{0\}$ and page $S^1 \times \{pt\} \times S^1$ in $T^3 \times \{1\}$. We think of τ_{23} as acting on the standard basis for $H_1(T^3, \mathbb{Z})$ via a permutation matrix $\sigma_{23} = \left(\begin{smallmatrix} 1 & 0 & 0 \\ 0 & 0 & -1 \\ 0 & 1 & 0 \end{smallmatrix}\right)$. By modifying the labelings in τ_{23}, we can draw trisections diagrams τ_{31} and τ_{12} of $T^3 \times [0,1]$ corresponding to 2-cycles $(3,1)$ and $(1,2)$ respectively.

Any matrix in $SL_3(\mathbb{Z})$ can be written as a product of permutation matrices (τ_{ij}) and matrices of the form $\left(\begin{smallmatrix} 1 & 1 & 0 \\ 0 & 1 & 0 \\ 0 & 0 & 1 \end{smallmatrix}\right)$ (special kind $f \times id_{S^1}$). Hece, equipped with the trisections τ_0 and τ_{ij} we can, in theory, draw $\star$-trisection diagrams for all the 4-manifolds $X_{F,g}$. The procedure of performing torus surgery becomes then a linear algebra problem. We will explain this explicitly by showing methods to trisect Logarithmic transforms and Luttinger Transforms.

Example 8.4 (Logarithmic transform). Let F be an embedded torus in X with self-intersection number zero. Fix a basis for $H_1(F, \mathbb{Z})$ and a trivialization $\eta(F) \cong T^2 \times D^2$. Following [3], given a matrix $A = \left(\begin{smallmatrix} a_{11} & a_{12} \\ a_{21} & a_{22} \end{smallmatrix}\right) \in SL_2(Z)$, we will denote as A-Logarithmic transform the 4-manifold $X_{F,A} = (X - \eta(F)) \cup_g (T^2 \times D^2)$, where $g : T^2 \times D^2 \to T^2 \times D^2$ is a homeomorphism given by the matrix $\left(\begin{smallmatrix} 1 & 0 & 0 \\ 0 & a_{11} & a_{12} \\ 0 & a_{21} & a_{22} \end{smallmatrix}\right)$. Suppose that F is in bridge position with respect to some trisection τ of X. Notice that

$$A = \begin{pmatrix} 0 & 0 & 1 \\ 0 & 1 & 0 \\ 1 & 0 & 0 \end{pmatrix} \cdot \begin{pmatrix} a_{22} & a_{21} & 0 \\ a_{12} & a_{11} & 0 \\ 0 & 0 & 1 \end{pmatrix} \cdot \begin{pmatrix} 0 & 0 & 1 \\ 0 & 1 & 0 \\ 1 & 0 & 0 \end{pmatrix}.$$

Thus to perform A-logarithmic transform along F we can take the $\star$-trisection $\widetilde{\tau}$ for the complement of F in X, and concatenate it with specific

trisections as follows,

$$X_{F,A} \quad : \quad \widetilde{\tau}\bigcup_{id}\tau_0\bigcup_{id}\tau_{31}\bigcup_{A\times id_{S^1}}\tau_{31}\bigcup_{id}\tau_{\emptyset}.$$

Here $\tau_\emptyset$ is the relative trisection for $T^2 \times D^2$ given by the empty diagram on a closed torus.

Integral logarithmic transform is given by the matrix $A_p = \left(\begin{smallmatrix} 0 & 1 \\ -1 & p \end{smallmatrix}\right)$. In particular 0-logarithmic transform is given by the map gluing map corresponding with the permutation $(2, 3)$ and so the trisection diagram for the 0-logarithmic transform $X_{F,0}$ can be simplified as follows:

$$X_{F,0} \quad : \quad \widetilde{\tau}\bigcup_{id}\tau_0\bigcup_{id}\tau_{23}\bigcup_{id}\tau_{\emptyset}.$$

Example 8.5 (Luttinger surgery). For an embedded torus F in X with self-intersection zero, a Luttinger surgery is an operation $X \mapsto X_{m,n}$ where $X_{m,n}$ is torus surgery along F via a homeomorphism given by the matrix $A_{m,n} = \left(\begin{smallmatrix} 1 & 0 & m \\ 0 & 1 & n \\ 0 & 0 & 1 \end{smallmatrix}\right)$. Since $A_{m,n}$ factors as follows,

$$A = \begin{pmatrix} 1 & 0 & 0 \\ 0 & 0 & 1 \\ 0 & 1 & 0 \end{pmatrix} \cdot \begin{pmatrix} 1 & m & 0 \\ 0 & 1 & 0 \\ 0 & 0 & 1 \end{pmatrix} \cdot \begin{pmatrix} 0 & 0 & 1 \\ 0 & 1 & 0 \\ 1 & 0 & 0 \end{pmatrix} \cdot \begin{pmatrix} 1 & n & 0 \\ 0 & 1 & 0 \\ 0 & 0 & 1 \end{pmatrix} \cdot \begin{pmatrix} 0 & 0 & 1 \\ 0 & 1 & 0 \\ 1 & 0 & 0 \end{pmatrix} \cdot \begin{pmatrix} 1 & 0 & 0 \\ 0 & 0 & 1 \\ 0 & 1 & 0 \end{pmatrix}.$$

We can preform Luttinger surgery along F, after fixing a trivialization $\eta(F) \cong T^2 \times D^2$ and a basis for $H_1(F, \mathbb{Z})$, by concatenating the following trisections.

$$X_{F,m,n} \quad : \quad \widetilde{\tau}\bigcup_{id}\tau_0\bigcup_{id}\tau_{23}\bigcup_{\left(\begin{smallmatrix} 1 & m \\ 0 & 1 \end{smallmatrix}\right)\times id}\tau_{13}\bigcup_{\left(\begin{smallmatrix} 1 & n \\ 0 & 1 \end{smallmatrix}\right)\times id}\tau_{13}\bigcup_{id}\tau_{23}\bigcup_{id}\tau_{\emptyset}.$$

Here, $\widetilde{\tau}$ is the $\star$-trisection for the complement of F and $\tau_\emptyset$ is the empty trisection diagram for $T^2 \times D^2$.

Appendix A. Classic diagrams

Let X be a $\star$-trisected 4-manifold with non-empty boundary. If the trisection is a classic relative trisection, the compression bodies given by the

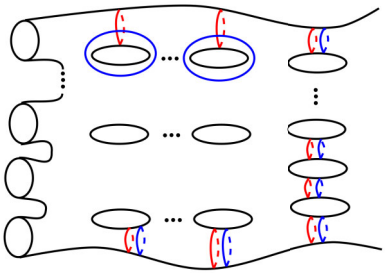

Figure A1: The standard picture for "classic" relative trisection diagrams.

pairwise intersection satisfy $C_i^0 = C_i^1$ for all $i = 1, 2, 3$. In particular, any diagram $(\Sigma; \alpha, \beta, \gamma)$ of such trisections satisfies that each pair of loops is slide equivalent to the loops like in Figure A1. In this case, there is a open book decomposition on ∂X induced by the trisection with binding having $b = |\partial\Sigma|$ components. In the existing literature algorithms have only been developed when the trisection surface has boundary ($b > 0$). The goal of this appendix is to extend these results to the case $b = 0$.

A.1. Relative trisections from Kirby diagrams

Let X be a connected 4-manifold with connected boundary. In [7] the authors showed how to draw a trisection diagram from a Kirby diagram of X if a page P for an open book decomposition of ∂X is given in the Kirby diagram. As expected, the proper modification of this result holds if P is the page of a fibration of ∂X over S^1; i.e., if $\partial P = \emptyset$. We will state the result in full generality.

Theorem A.1 (Adaptation from Main Theorem of [7]). Take a handle decomposition of X with one 0-handle, some 1-handles, 2-handles and 3-handles described explicitly in the form of a Kirby diagram. Let P be the page of an open book decomposition **or** a fibration over S^1 of ∂X. Suppose that P is explicitly drawn in the Kirby diagram. Then there is an algorithm to draw a trisection diagram for X described as follows:

1) Isotope P in the diagram so that P has a 2-dimensional handle decomposition induced by the 0-handle and some 1-handles **and 2-handles** of X. You might need to add 1/2-cancelling pairs to do so.

2) If not all the 1-handles of X were used to build P, add genus to P by tubing it as in Figure A2. Call this new surface $\widetilde{\Sigma}$.

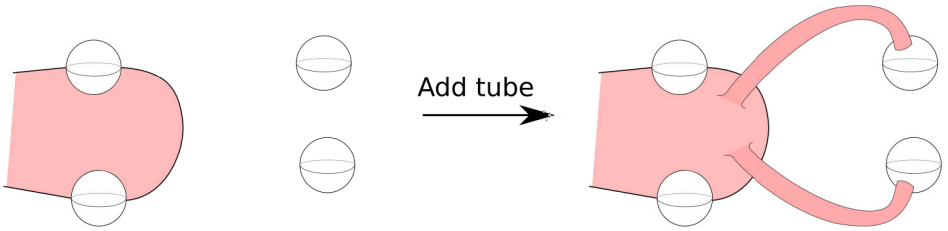

Figure A2: Tubing the page.

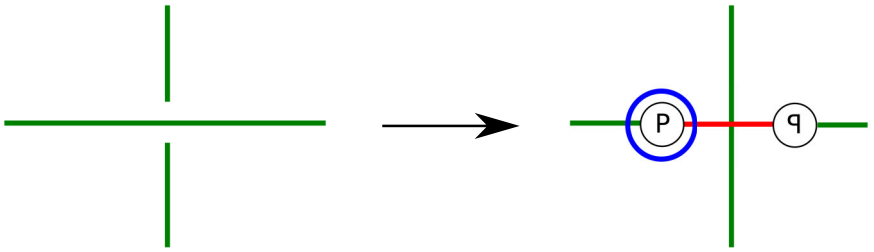

Figure A3: How to fix a crossing.

3) Project the attaching regions of the rest of the 2-handles onto $\widetilde{\Sigma}$. With the help of Reidemeister I moves ensure that the framing of the handles is given by the surface; and use Reidemeister II moves to ensure that every loop has at least one overcrossing in the link projection.

4) Stabilize $\widetilde{\Sigma}$ so that the link above has no crossing following Figure A3. Call this new surface Σ. Let γ be the loops in Σ arising from the link projection, let α and β be the red and blue curves in Σ coming from the stabilizations.

5) By construction $|\alpha| = |\beta| \geq |\gamma|$. If the inequality is strict, we do the following: For each component γ_i, by construction we can pick a loop β_{J_i} intersecting γ_i transversely in one point and disjoint from other γ curves. Take a β_j not in the selected set $\{\beta_{J_i}\}_i$; β_j intersects a unique γ curve in one point, say γ_{i_0}. Slide β_j over $\beta_{J_{i_0}}$ using an arc of γ_{i_0}; denote the resulting curve by γ_j.

The tuple $(\Sigma; \alpha, \beta, \gamma)$ is a relative trisection diagram for X inducing the given fibration on the boundary.

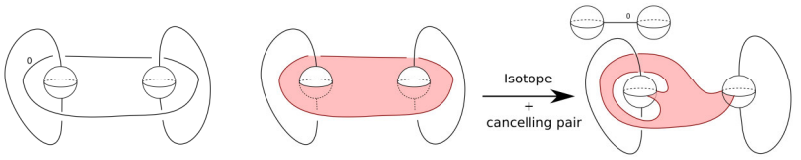

Figure A4: Left: A Kirby diagram for the complement of the unknotted torus in S^4. Right: The shaded surface is an embedding of a torus page for the fibration of T^3.

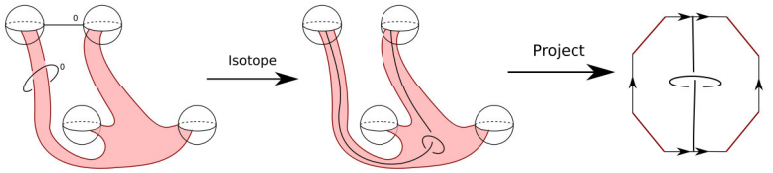

Figure A5: After sliding, notice that the page has a handle decomposition induced by the 0-handle, the pair of 1-handles and one 2-handle of the 4-manifold.

Proof. The decomposition of X will be given as follows: Divide the 2-handles of X by $h^2 = h^2_P \cup h^2_r$ where h^2_P are the ones used to build P and h^2_r the rest of the 2-handles. Define $X_1 = B^4[h^1 \cup h^2_P]$. We can see Σ as embedded in ∂X_1 by stabilizing the standard circular decomposition in ∂X_1 as in Subsection 3.4, say

$$\partial X_1 = \Big(C_\alpha \cup_\Sigma C_\beta\Big) \Big/ \Big(\partial_- C_\alpha =_{id} \partial_- C_\beta\Big).$$

Define $X_2 = \eta_X(C_\beta)[h^2_r]$ and $X_3 = X - int(X_1 \cup X_2)$. The proof that $X = X_1 \cup X_2 \cup X_3$ is indeed a relative trisection is the same as in Theorem 1 of [7]. □

Example A.2. Figures A4, A5 and A6 describe how to draw a relative trisection diagram for the complement of an unknotted torus in S^4.

Example A.3. Figures A7 and A8 show how to trisect the thickened 3-torus $T^3 \times [0,1]$ in such a way that on one side the S^1-foliation has fiber $S^1 \times S^1 \times \{pt\}$ and in the other boundary the fiber is $S^1 \times \{pt\} \times S^1$.

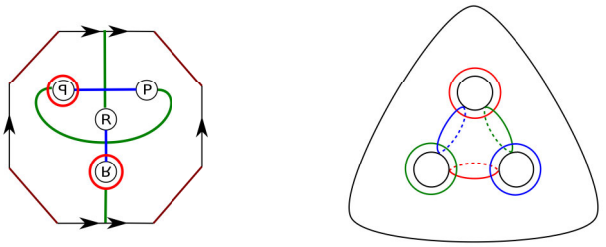

Figure A6: By resolving the crossings as in Step 4, since we have the same number of loops of each color, we obtain a relative trisection diagram for X (left). We get the diagram in the right by a diffeomorphism of the surface.

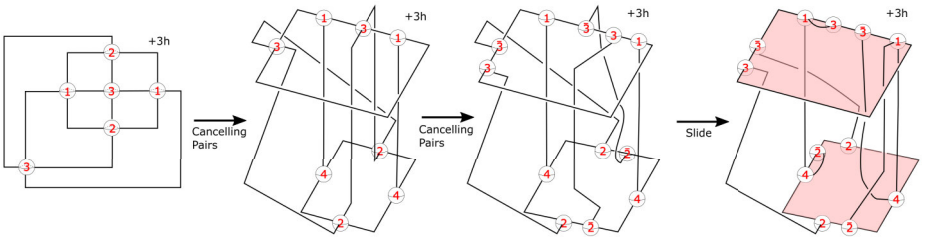

Figure A7: A Kirby diagram for $T^3 \times [0,1]$ obtained by thickening a Heegaard diagram for the 3-torus. After adding a 1/2-cancelling pair, you can see two embedded tori (shaded in pink) corresponding to S^1-fibers $T_{12} = S^1 \times S^1 \times \{pt\} \times \{0\}$ and $T_{13} = S^1 \times \{pt\} \times S^1 \times \{1\}$. Notice that the pages T_{12} and T_{13} have handle decompositions induced by the 0-handle, the 1-handles and some 2-handle of the 4-manifold.

A.2. The monodromy induced on ∂X

In [5], the authors described an algorithm to compute the monodromy of an open book decomposition induced by a trisection when the diagram has boundary ($b > 0$). If the trisection surface is closed, the trisection will induce a fibration over S^1 and the monodromy can also be computed following a suitable modification of the original algorithm. We now describe the algorithm in general. The key idea is to take properly embedded 1-manifolds in the trisection surface that cut a page into a disk and traverse the boundary of the trisection using the correct handle slides.

Theorem A.4 (Adaptation from of Theorem 5 of [5]). A relative trisection diagram encodes an open book decomposition or a fibration over S^1

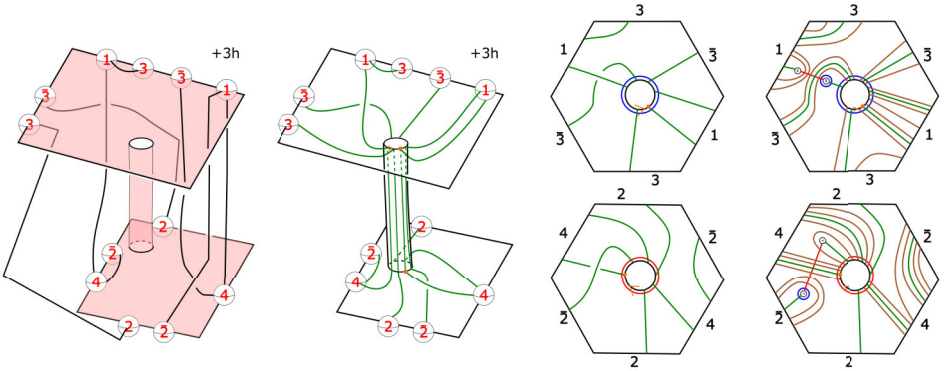

Figure A8: After tubing the two tori, we draw a link diagram for the rest of the 2-handles in a genus two surface. By resolving the crossings as in Step 4, we obtain a diagram with fewer γ-curves (green). We perform Step 5 in order to find γ_3 (brown). This final result is a relative trisection diagram for $T^3 \times [0,1]$ with S^1-fibers on its boundary given by $T_{12} = S^1 \times S^1 \times \{pt\} \times \{0\}$ and $T_{13} = S^1 \times \{pt\} \times S^1 \times \{1\}$.

on ∂X with page given by Σ_α, the surface resulting from Σ by compressing along the α curves, and monodromy $\mu : \Sigma_\alpha \to \Sigma_\alpha$ determined as follows:

1) Choose an ordered collection of properly embedded arcs or[9] simple closed curves a on Σ, disjoint from α and such that the corresponding 1-manifolds in Σ_α cut Σ_α into a disk[10].

2) There exists a collection of properly embedded 1-manifolds a_1 and simple closed curves β' in Σ such that (α, a_1) is handle slide equivalent to (α, a), β' is handle slide equivalent to β, and a_1 and β' are disjoint. We claim that in this step we do not need to slide α curves over α curves, only a 1-manifolds over α curves and β curves over β curves. Choose such an a_1 and β'.

3) There exists a collection of properly embedded 1-manifolds a_2 and simple closed curves γ' in Σ such that (β', a_2) is handle slide equivalent to (β', a_1), γ' is handle slide equivalent to γ, and a_2 and γ' are disjoint. Again we claim that we do not need to slide β' curves over β' curves. Choose such an a_2 and γ'.

[9]We could have both arcs and curves simultaneously.
[10]As many disks as boundary components of X.

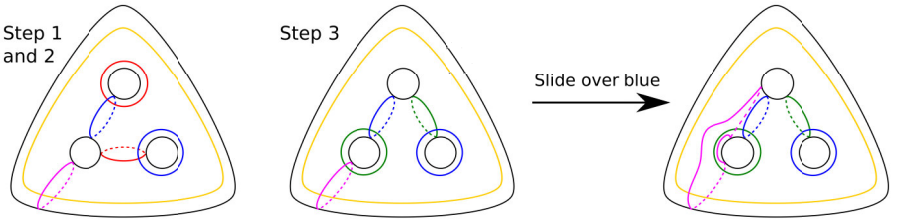

Figure A9: Left: The outer pair of curves (yellow and pink) correspond to the 1-manifolds $a = a_1$ disjoint from the α (red) and β (blue) loops. Right: After switching to the β, γ (green) pair, we need to slide a_1 over β to get 1-manifolds disjoint from γ, we call those a_2.

4) There exists a collection of properly embedded 1-manifolds a_3 and simple closed curves α' in Σ such that (γ', a_3) is handle slide equivalent to (γ', a_2), α' is handle slide equivalent to α, and a_3 and α' are disjoint. Again we claim that we do not need to slide γ' curves over γ' curves. Choose such an a_3 and α'.

5) The pair (α', a_3) is handle slide equivalent to (α, a_*) for some collection of 1-manifolds. Choose such an a_*. Note that now a and a_* are both disjoint from α and thus we can compare the corresponding 1-manifolds in Σ_α.

6) The monodromy μ is the unique map (up to isotopy) such that

$$\mu(\varphi_\alpha(a)) = \varphi_\alpha(a_*),$$

respecting the ordering of the 1-manifolds.

Proof. The proof is the same as in Theorem 5 on [5]. The only observation is that the proof of Lemma 13 of [5], a key lemma for this result, does not apply when Σ_α is closed. This problem can be solved by considering the annulus $a \times [-1, 1]$ for any loop in P instead of the disk in the proof of Lemma 13. The proof then works. □

Example A.5. Figures A9, A10 and A11 show how to run the algorithm for the monodromy in the concrete case of the trisection of the complement of the unknotted torus in S^4.

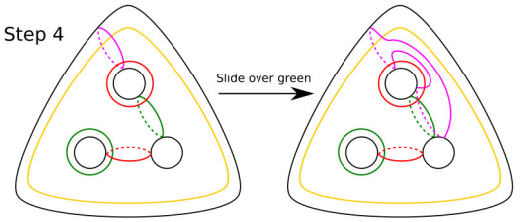

Figure A10: After isotopy of a_2 and drawing now the pair (γ, α), we slide a_2 over γ to get 1-manifolds disjoint from α, we call those $a_3 = a_*$.

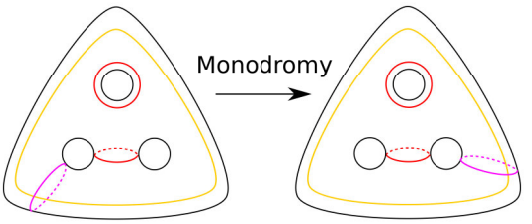

Figure A11: The orientation preserving monodromy is defined in the torus obtained by compressing along the α loops and its determined by $a \mapsto a_*$. Notice that in this case we obtained the identity map, as expected.

Acknowledgements

The authors of this paper are grateful to the referee and Maggie Miller for their comments on the previous draft. The first author would like to thank Jeff Meier and the topology group of the University of Iowa for helpful conversations. The second author would like to thank the Max Planck Institute for Mathematics, and Steve Hamborg, for their hospitality.

References

[1] A. Abrams, D. Gay, and R. Kirby, *Group trisections and smooth 4–manifolds*, Geometry & Topology **22** (2018), no. 3, 1537–1545.

[2] S. Akbulut, 4-Manifolds, Vol. 25, Oxford University Press (2016).

[3] R. I. Baykur and N. Sunukjian, *Round handles, logarithmic transforms and smooth 4-manifolds*, Journal of Topology **6** (2013), no. 1, 49–63.

[4] L. C., *Surfaces bounding the unlink*, Mich. Math J. (1982), no. 3, 289–298.

[5] N. Castro, D. Gay, and J. Pinzón-Caicedo, *Diagrams for relative trisections*, Pacific Journal of Mathematics **194** (2018), no. 2, 275–305.

[6] N. A. Castro, *Trisecting smooth 4-dimensional cobordisms*, preprint, `arXiv:1703.05846`, (2017).

[7] N. A. Castro, D. T. Gay, and J. Pinzón-Caicedo, *Trisections of 4-manifolds with boundary*, Proceedings of the National Academy of Sciences **115** (2018), no. 43, 10861–10868.

[8] N. A. Castro, G. Islambouli, M. Miller, and M. Tomova, *The relative $\mathcal{L}$-invariant of a compact 4-manifold*, preprint, `arXiv:1908.05371`, (2019).

[9] N. A. Castro and B. Ozbagci, *Trisections of 4-manifolds via Lefschetz fibrations*, Mathematical Research Letters **26** (2019), no. 2, 383–420.

[10] T. Etgü and B. Ozbagci, *Explicit horizontal open books on some plumbings*, International Journal of Mathematics **17** (2006), no. 9, 1013–1031.

[11] P. Feller, M. Klug, T. Schirmer, and D. Zemke, *Calculating the homology and intersection form of a 4-manifold from a trisection diagram*, Proceedings of the National Academy of Sciences **115** (2018), no. 43, 10869–10874.

[12] R. Fintushel and R. J. Stern, *Knots, links, and 4-manifolds*, Inventiones mathematicae **134** (1998), no. 2, 363–400.

[13] V. Florens and D. Moussard, *Torsions and intersection forms of 4-manifolds from trisection diagrams*, preprint, `arXiv:1901.04734`.

[14] D. Gay and R. Kirby, *Trisecting 4–manifolds*, Geometry & Topology **20** (2016), no. 6, 3097–3132.

[15] D. Gay and J. Meier, *Doubly pointed trisection diagrams and surgery on 2-knots*, preprint, `arXiv:1806.05351`, (2018).

[16] C. Hayashi and K. Shimokawa, *Heegaard splittings of the trivial knot*, Journal of Knot Theory and Its Ramifications **7** (1998), no. 8, 10731086.

[17] S. Kim and M. Miller, *Trisections of surface complements and the Price twist*, preprint, `arXiv:1805.00429`, (2018).

[18] R. Kirby, *Trisections of 4-manifolds*, Proceedings of the National Academy of Sciences **115** (2018), no. 43, 10853–10856.

[19] D. Koenig, *Trisections of 3-manifold bundles over S^1*, preprint, arXiv:1710.04345, (2017).

[20] P. Lambert-Cole and J. Meier, *Bridge trisections in rational surfaces*, preprint, arXiv:1810.10450, (2018).

[21] J. Meier, *Trisections and spun four-manifolds*, Mathematical Research Letters **25** (2018), no. 5, 1497–1524.

[22] J. Meier and A. Zupan, *Bridge trisections of knotted surfaces in S^4*, Transactions of the American Mathematical Society **369** (2017), no. 10, 7343–7386.

[23] ———, *Genus-two trisections are standard.*, Geometry & Topology **21** (2017), no. 3, 1583–1630.

[24] ———, *Bridge trisections of knotted surfaces in 4-manifolds*, Proceedings of the National Academy of Sciences **115** (2018), no. 43, 10880–10886.

[25] J.-P. Otal, *Présentations en ponts du noed trivial*, C. R. Acad. Sci. Paris Sér. I Math **294** (1982), no. 16, 553–556.

[26] F. Waldhausen, *Heegaard-zerlegungen der 3-sphäre*, Topology **7** (1968), no. 2.

Department of Mathematics and Statistics, Binghamton University
4400 Vestal Parkway E, Binghamton, NY 13902, USA
E-mail address: jaranda@binghamton.edu

Mathematics, University of Nebraska-Lincoln
1144 T St, Lincoln, NE 68588, USA
E-mail address: jesse.moeller@huskers.unl.edu

Received December 11, 2019
Accepted November 23, 2020